AFRL-AFOSR-UK-TR-2012-0007

Gas Detection using Hyperthermal Images

Dan G Blumberg

Ben Gurion University
Geography and Environmental Development
Ben-Gurion Blvd.
Beer-Sheva, Israel 84105

EOARD GRANT 08-3056

Report Date: November 2011

Final Report for 26 September 2008 to 26 September 2011

Air Force Research Laboratory
Air Force Office of Scientific Research
European Office of Aerospace Research and Development
Unit 4515 Box 14, APO AE 09421

REPORT DOCUMENTATION PAGE

Form Approved OMB No. 0704-0188

1. REPORT DATE *(DD-MM-YYYY)*	2. REPORT TYPE	3. DATES COVERED *(From – To)*
28-Mar-2012	Final Report	26 September 2008 – 26 September 2011

4. TITLE AND SUBTITLE

Gas Detection using Hyperthermal Images

5a. CONTRACT NUMBER

FA8655-08-1-3056

5b. GRANT NUMBER

Grant 08-3056

5c. PROGRAM ELEMENT NUMBER

61102F

6. AUTHOR(S)

Professor Dan G. Blumberg

5d. PROJECT NUMBER

5d. TASK NUMBER

5e. WORK UNIT NUMBER

7. PERFORMING ORGANIZATION NAME(S) AND ADDRESS(ES)

Ben Gurion University
Geography and Environmental Development
Ben-Gurion Blvd.
Beer-Sheva Israel 84105

8. PERFORMING ORGANIZATION REPORT NUMBER

N/A

9. SPONSORING/MONITORING AGENCY NAME(S) AND ADDRESS(ES)

EOARD
Unit 4515 BOX 14
APO AE 09421

10. SPONSOR/MONITOR'S ACRONYM(S)

AFRL/AFOSR/RSW (EOARD)

11. SPONSOR/MONITOR'S REPORT NUMBER(S)

AFRL-AFOSR-UK-TR-2012-0007

12. DISTRIBUTION/AVAILABILITY STATEMENT

Approved for public release; distribution is unlimited.

13. SUPPLEMENTARY NOTES

14. ABSTRACT

The research here has been divided into three parts. We started with gases being emitted from a smokestack. Not knowing what gasses were being emitted, we developed a way to correlate known laboratory spectra with the emitted spectra. We found the two main components: carbon dioxide and sulfur dioxide. Our method for doing this involved the careful selection of critical wavelengths for the analysis.

While this enabled us to find the main concentrations of gas, we wanted to extend the physical extent of the cloud. We did this by shifting from the laboratory signatures to the actual averaged real data signatures of the gas cloud and then performing a matched filter. The image was then thresholded on the basis of the background statistics. This procedure was performed iteratively until a stable division of background/gas was achieved.

The resulting signatures can be separated by energy into that which is due to the gases and that which due to the background; the percentages of each gas can be calculated. Finally, we successfully separated the temperature from the gas by recognizing the different temperature dependences of the gas components.

In this report, we develop an algorithm for the detection, identification and relative quantification of effluent gases emitted from an industrial plume stacks using an LWIR hyperspectral remote sensing system. The algorithm is based on applying a stepwise regression process using known library gas signatures when analyzing experimental data. The system first fits the spectra to a combination of all the possible gases; it then systematically reduces the number of gases while maintaining a good fit to the observed spectra.

The system was tested on data cubes synthesized in the Digital Imaging and Remote Sensing (DIRS) Laboratory at the Rochester Institute of Technology and on actual gas cubes measured from the stack of a power plant; good results were obtained.

An extension of our algorithm for the stepwise detection of gases is considered. In particular, we tackle the problem of gases which resemble other gases, i.e., often when gases a and b are detected in a gas cloud, only a is present, while b simply looks like a. In our new algorithm, a prior analysis shows which gases can be confused with each other; thresholds are set to avoid multiple gas identifications of a single gas.

15. SUBJECT TERMS

EOARD, Hyperspectral Imagery, Image Processing

16. SECURITY CLASSIFICATION OF:			17. LIMITATION OF ABSTRACT	18, NUMBER OF PAGES	19a. NAME OF RESPONSIBLE PERSON
a. REPORT	b. ABSTRACT	c. THIS PAGE			A. GAVRIELIDES
UNCLAS	UNCLAS	UNCLAS	SAR	48	19b. TELEPHONE NUMBER *(Include area code)* +44 (0)1895 616205

Final Report for EOARD

Contract No. FA8655-08-1-3056

Research Title: Gas Detection using Hyperthermal Images

Prof. Dan G. Blumberg and Prof. Stanley Rotman

November 2011

Final Report on Gas Detection for EOARD
Covering the years 2008-2011

Dan Blumberg and Stanley Rotman
Ben-Gurion University of the Negev

Nov. 4, 2011

The following report is the summary and culmination of three years of research on Gas Detection at Ben-Gurion University of the Negev from 2008 to 2011.

The basic data consisted of hyperspectral cubes taken of the Haifa Refinery with the TELOPS sensor, and DIRSIG simulations provided by the Rochester Institute of Technology. The spectral information consisted of LWIR (Long Wave Infrared) spectra from 8-12 microns.

The research can be summarized as falling into two basic areas. In the first, we experimented with real gas data determining our ability to detect the parameters of the CO_2 and SO_2 present in the image. These gases were chosen because, without any unmixing of the spectra, they were clearly visible in pixels immediately adjacent to the top of the stacks. Our research emphasized determining the physical extent of the CO_2 and SO_2 cloud and separating the temperature and the concentration effects. This work has been summarized in the attached paper by L. Sagiv et al.

In the second area of research, we extended an RIT step-wise regression algorithm for taking pixels of mixed gases in our datasets and separating them into gases defined by a spectral library. The initial RIT algorithm had only been used to find single gases in known areas of the image. We extended this work to include multiple gases mixed together and to determine which pixels had or didn't have gases at all. We determined that the initial algorithm was not adequate, and that a "shift" algorithm forcing a gas signature to fit a particular signature was necessary. This was applied to both the real and synthetic imagery that we had available. This work has been summarized in the attached paper by D.N. Rotman et al.

Innovative algorithms have been developed to determine the following:

1. We have shown an iterative process to determine the furthest extent of a gas cloud once an initial limited number of pixels have been identified with this gas.
2. We have separated the temperature and concentration effects in our imagery by developing a model to explain the difference in temperature dependence of the CO_2 and SO_2 gas signatures.

3. We have shown how to avoid false identifications of the gases using the RIT algorithm by "toughening" the criteria for determining a gas is present. This is done by a fitting algorithm of the laboratory signature to the actual data with is performed after the stepwise regression algorithm
4. We have considered explicitly the possibility that if two or more gases have been detected in a pixel that these gases may be easily confused one for another. Higher thresholds are applied for the joint detection of "similar" gases.

While not directly being funded by this project, we have been looking into atmospheric correction of the gas signatures. This work will be passed on to AFRL when it is completed.
The two attached papers summarize this research. We thank EOARD and AFRL for the opportunity to do this research.

Gas detection from smoke stacks: an iterative approach with emphasis on good wavelength selection

Lior Sagiv, Stanley R. Rotman and Dan G. Blumberg
Ben-Gurion University of the Negev

Submitted to: Remote sensing of environment
Date of submission: _____
Number of text pages: ____18_____
Number of figures:_____33_____
Address editorial comments to Dan G. Blumberg, Department of Geography and Environmental Development, Ben-Gurion University of the Negev, Blumberg@bgu.ac.il

ABSTRACT

In this paper, we present the development of an algorithm for the detection, identification and relative quantification of effluent gases emitted from an industrial plume stacks using an LWIR hyperspectral remote sensing system. The technique consists of the localization of critical wavelengths in the spectral signatures and their integration into an algorithm for the detection of high concentrated gas pixels in the image cube using a correlation coefficient metric. Further mapping of low concentrated pixels is executed by an iterative Matched Filter (MF) method. Of crucial importance is our ability to separate those pixels which have been contaminated by the gas from those which have not (or when the concentration is lower than the threshold) when evaluating the statistics of the background. Following the mapping of pixels with gas in the image cube, a least squares method is applied to derive the gas concentration. We successfully separate temperature and concentration effects from each other. The algorithm was tested on data cubes acquired in the bay of Haifa with chimneys emitting SO_2 and CO_2 gases. The images were acquired from distances of 400 and 1700 meters; good results were obtained.

Index Terms – Hyperspectral, Gas, Detection, Long Wave Infrared

I. **Introduction**:

Environmental problems stemming from the pollution emitted by industrial effluent gas stacks are common to all countries since the 17th century when the first industrial chimneys were built. Flue stacks are vertical pipes, chimneys, through which combustion product gases called flue gases are exhausted to the outside air (Douet 1988). Atmospheric models are required to simulate the dispersion of pollutants from such stacks and few technologies are available to monitor these pollutants. The advent of multispectral and hyperspectral sensors lead to the ability to obtain three-dimensional data for many scenarios: subpixel point target detection, multi-pixel anomaly detection and large scale gas detection (Shaw & Burke 2003). For each of these applications, there is a tendency to believe that "more is better": a larger number of wavelengths will provide better results than a smaller number. Some researchers will add the caveat that since the Signal to Noise Ratio (SNR) goes down for each channel as the available bandwidth is split into more and more partitioned bands, there is an optimum number of bands that should be used. However, even if the SNR is not decreased, there is reason to believe that the addition of too many bands may itself decrease performance.
The gas detection project we are working on presently has begun by concentrating on this problem: determining how many and which bands are the best wavelengths for detecting the presence of a gas. Effluent gases such as those associated with industrial activity are well characterized by their LWIR absorption features (Czerwinski et al., 2005). We present results on two datacubes of power plant smoke stacks taken by the FIRST sensor in two ranges – 400 and 1700m away (Farley et al., 2006). We will show that we can well identify the two major gas signatures in the stack plume by focusing on the wavelengths for which the gas signature is maximum and minimum.

The initial mapping enables the definition of a new reference signature for a wider detection of the gas in the image. This signature is estimated from the actual signatures in the cube itself; the covariance matrix of the background is determined iteratively by eliminating pixels which have been contaminated by the gas signatures. This is highly significant since Theiler et al. (2006) have shown that pixels ostensibly from the background but containing gas content can potentially affect the evaluation of the statistics of the background. The target signature is integrated into a Matched filter (MF) which provides wider detection coverage. The identified pixels gas content can then be quantified by a least-squares algorithm which curve fits the identified gas spectral signatures to the experimentally measured pixels. A new technique is developed which allows for the calculation of the temperature and concentration separately.

The paper is organized as follows: in Section II, we describe the basic experimental set up and the initial identification of the emitted gases. The spatial extent of the gases is explored in Section III; the relative quantitative evaluation of the concentration of the gases is given in Section IV. The temperature and concentration effects are separated in Section V. We summarize the results in Section VI.

II. Gas Detection: Single datacube of a smokestack:

a. Goal:

We are given a set of datacubes in the Long Wave Infrared (LWIR) (Fig.1). The data cubes were attained during an experiment at the bay of Haifa, Israel, using the "FIRST" spectral imager. The sensor was developed by Telops; it's a LWIR hyperspectral imager based on FTIR technology (Farley et al., 2006). The FIRST provides datacubes of up to 320x250 pixels at 0.35 mrad spatial resolution over the 8-12 micron spectral range and with spectral resolutions of up to 0.25 cm^{-1}. In the experiment, the FIRST imaged chimneys from distances of 400m and 1700 m away at a rate of 1 Hz per datacube.

Fig. 1. Sample frame of gases emitted from the smoke stack

The gases being emitted were unknown. However, a reasonable guess from known laboratory signals implies that CO_2 and SO_2 were probably major components. The following graphs show the laboratory signatures for CO_2 (Fig. 2), SO_2 (Fig. 3), and a fit to an actual pixel signature taken from the data (Fig. 4).

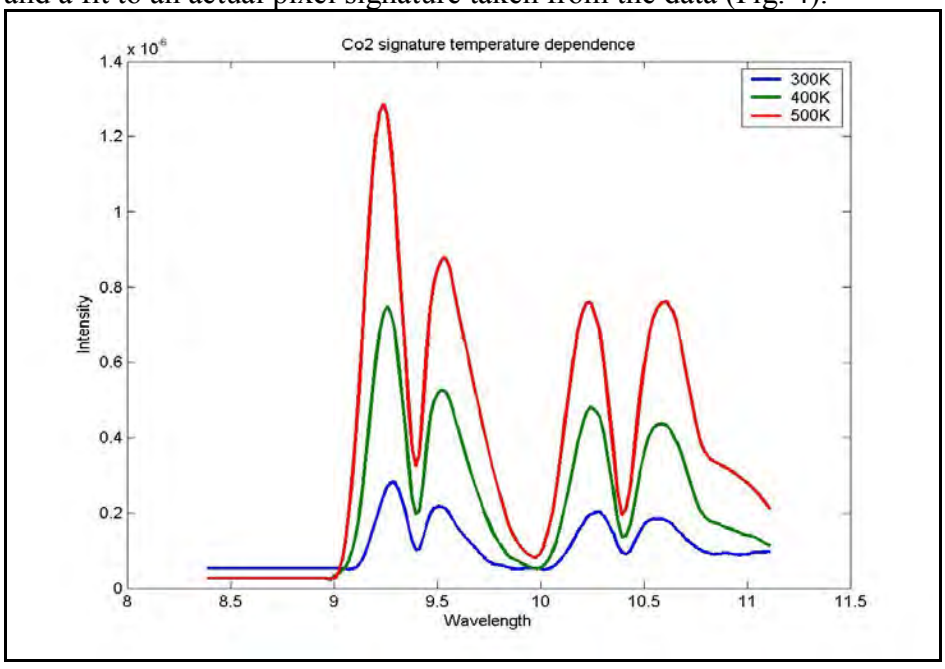

Fig. 2: The curves represents laboratory signatures of CO_2 at various temperatures.

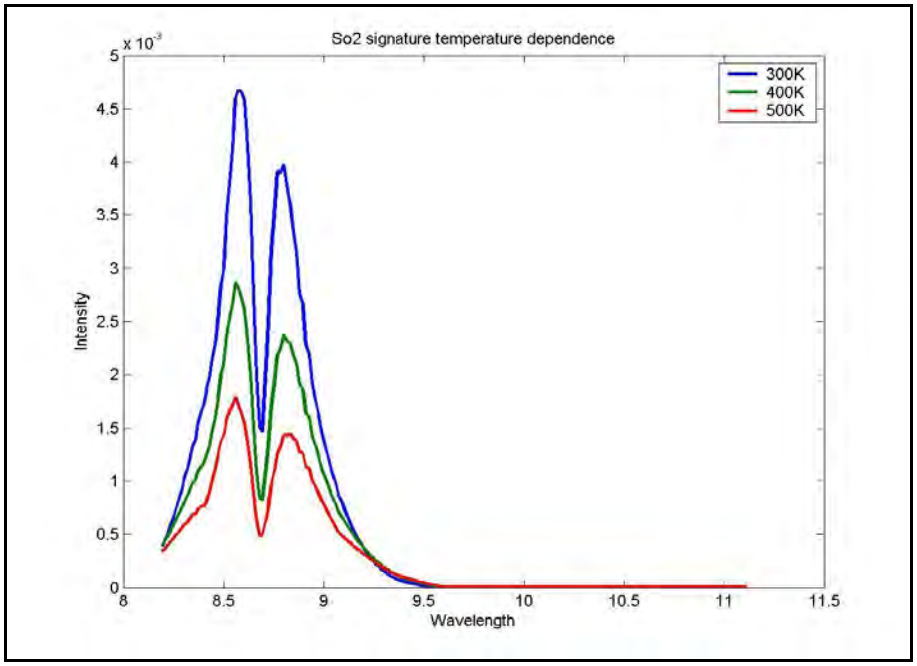

Fig. 3: The curves represent a laboratory signature of SO_2 at various temperatures.

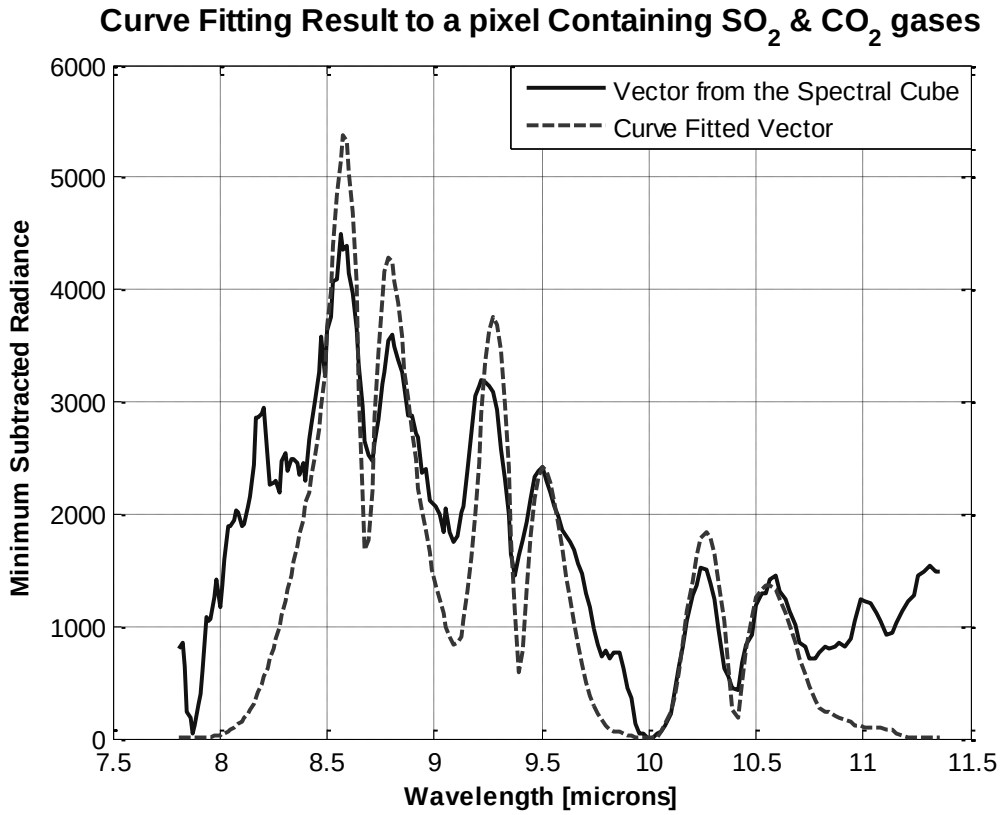

Fig. 4: An actual gas pixel taken from the datacube (bold curve). Also shown is a fit to the weighted sums of the CO_2 and SO_2 laboratory signatures as will be described later in the text (dashed curve). Note that all the peaks in the laboratory curves seem to correspond to peaks in the actual data. The converse is, however, not true; additional unexplained peaks can be found in the real data.

To mathematically determine if a particular type of gas is present in the experimental signature, we decided to correlate the laboratory signature with the measured results, calcuting the standard correlation coefficient between the two vectors. We note that the spectra of the two gases are quite dissimilar and do not overlap. Thus, we can expect to be able to identify both of them easily. We take the maxima and minima points of the theoretical gas signal; we will use the wavelengths of these points and the wavelengths between these points that have the average values of the maxima and the minima (Fig. 5). By limiting which wavelengths are used in the correlation, we avoid interactions with extraneous peaks and gases that may be present in the signature.

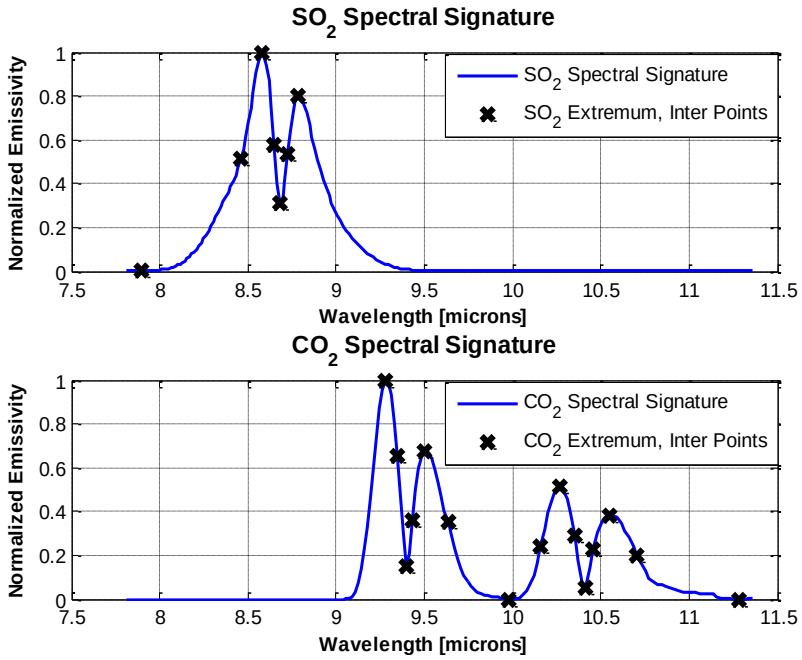

Fig. 5: Wavelength selection for the correlation fit of the suspected data to the library signatures

III. **Spatial determination of the gas cloud**:
   a. Initial estimate of gas cloud extent

We can now take these signatures and test the cubes which we have available for target detection. The cubes were taken from two distances: 400 meters and 1,700 meters. Multiple cubes at each distance were taken; the following results were substantiated over all the cubes.

The left sides of Figs. 6 and 7 shows the correlation coefficients of the two gases with the output of the smoke stacks. On the right, we show a binary image indicating where the coefficients exceed a 0.8 threshold.

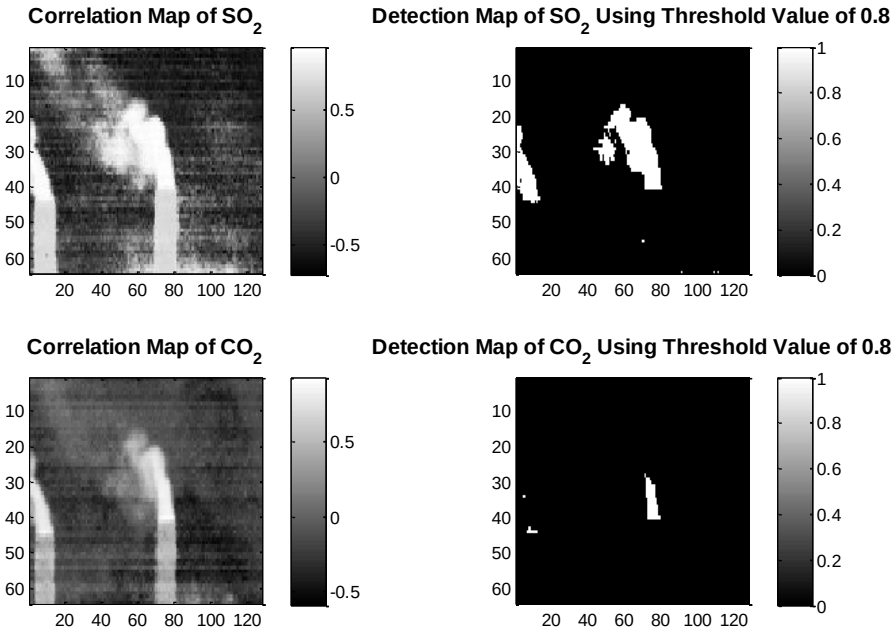

Fig. 6: Correlation map for gases from the smokestack at 400 meter distance.

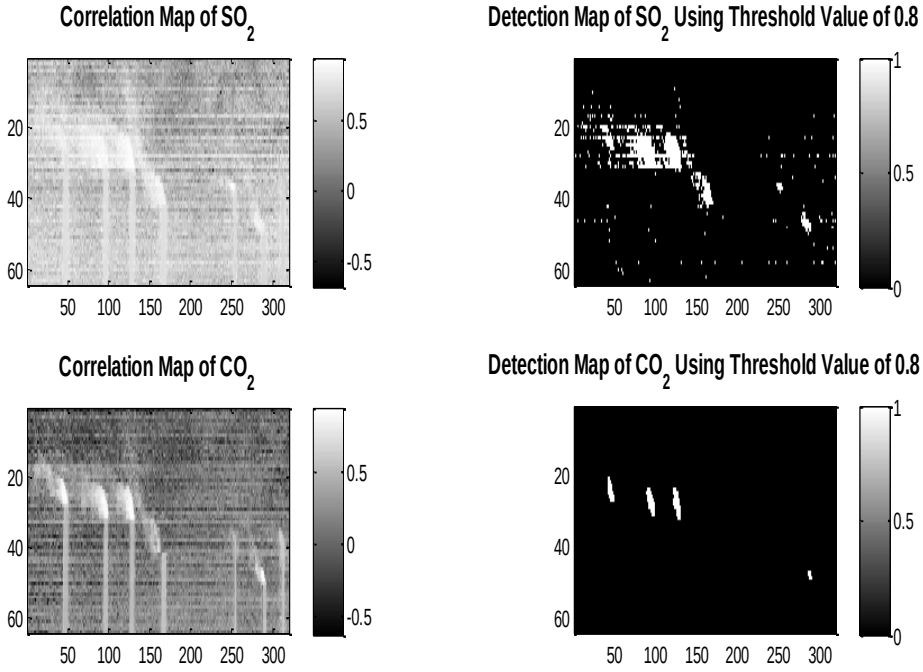

Fig. 7: Correlation Map for gases from the smokestack at 1700 meter distances.

When the same procedure was applied to the images with the spectra of the other gases, no detections were obtained.

b. Extension of method to real (non laboratory) signatures:

While these results are rather exciting, there is still a certain weakness to the results. We have to rely on a laboratory signature for matching the gas. This signature could

be altered by either sensor or atmospheric anomalies (Kopeika 1998, Manolakis & Shaw 2002, Figov 2007); in fact, the atmosphere will almost definitely have a dominant effect.

If we have already determined which pixels definitely have the gas we are interested in, we should be able to use the data itself iteratively to determine an even better signature for the gas. The initial mapping (of highly concentrated gas pixels) enables the definition of a new reference signature which is more suitable for a wider detection of the gas in the image comparable to the initial spectral signature.

The following procedure was applied:

1. The laboratory signature was correlated with each pixel; the image was then segmented with a high correlation coefficient threshold to detect pixels that definitely had the gas.
2. The pixels thus determined were spatially filtered with a median filter to only choose genuine gas pixels. (Fig. 8)
3. Determining a new signature: We average the signatures of those pixels which have been determined to be high concentrations of gas.
4. This signal is then used in a matched filter to once again attempt to find low concentration pixels. The equation for the matched filter would be:

$$MF\left(\vec{r}\right)=\frac{\left(\vec{s}-\vec{\mu}\right)^{T}\mathbf{C}^{-1}\left(\vec{r}-\vec{\mu}\right)}{\left(\vec{s}-\vec{\mu}\right)^{T}\mathbf{C}^{-1}\left(\vec{s}-\vec{\mu}\right)} \qquad (1)$$

where

$\vec{r}$ - is the measured pixel
$\vec{s}$ - is the signal of a pixel with gas
$\vec{\mu}$ - is the signal of a pixel without gas
$\mathbf{C}^{-1}$.- is the inverse covariance matrix of the background.

For the wavelengths to be chosen here, we defined and used the Maximum Spectral Information Criteria. This consists of examining the spectra of the gas we were interested in, and only using those wavelengths which were directly related. This was done by integrating the gas spectrum over the entire wavelength band being measured; the wavelengths which contribute between a lower minimum (0.05) and a higher maximum (0.95) are used. (See Figs. 9a and 9b).

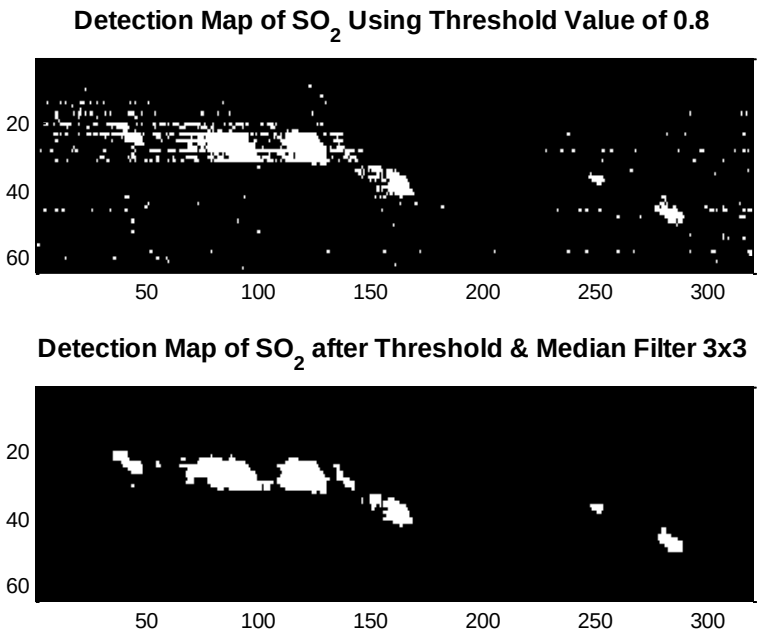

Fig. 8: Median filtering the detection mapy for SO_2.

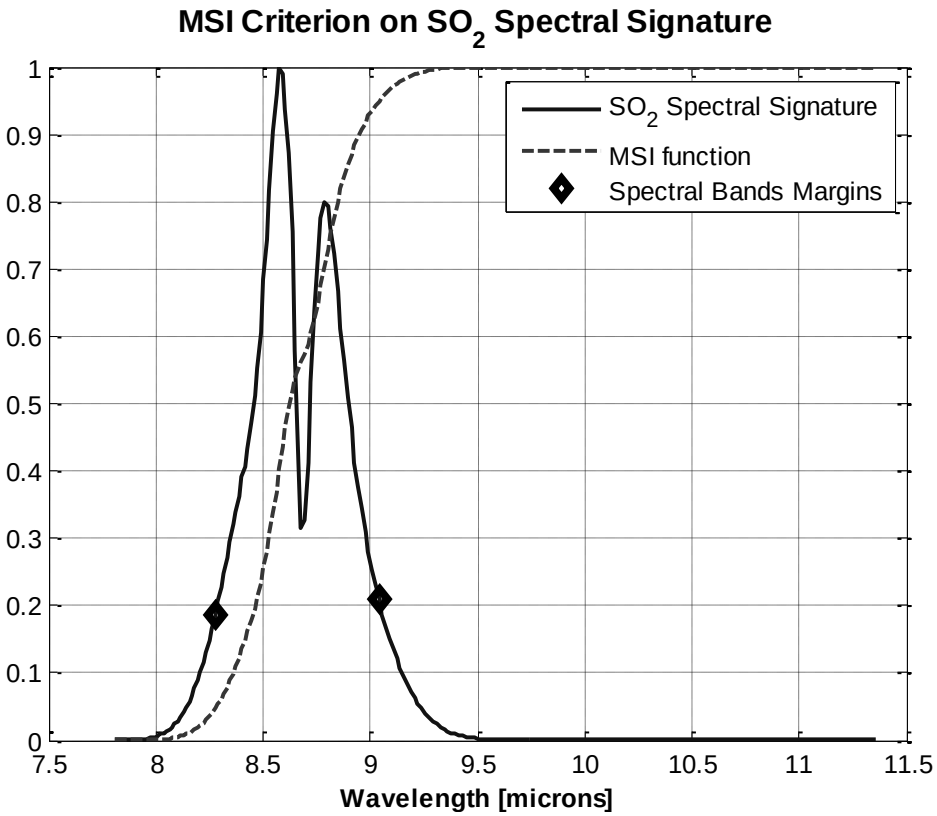

Fig. 9a: Dashed curve is the integral of the spectrum of SO_2 (and referred to as the MSI spectral signature).. The wavelengths between 0.05 and 0.95 (as measured on the MSI function) will be used.

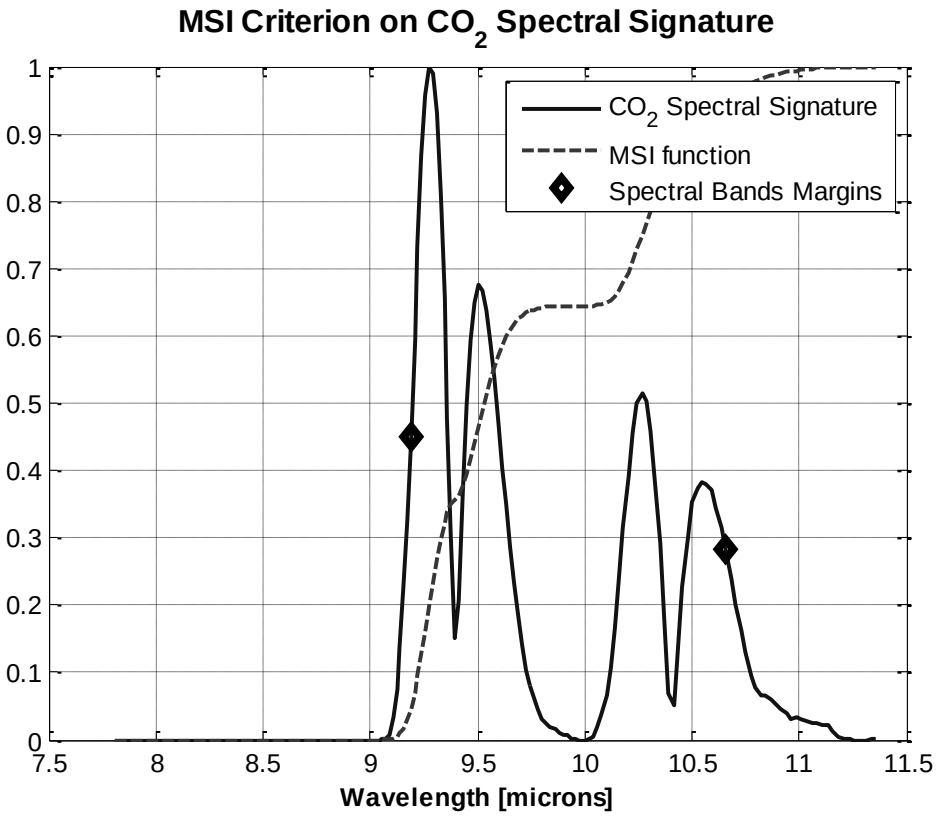

Fig. 9b: Dashed curve is the integral of the spectra of CO_2 (and referred to as the MSI spectral signature). The wavelengths between 0.05 and 0.95 (as measured on the MSI function) will be used.

As stated above, the signal in Equation 1 will be found by thresholding the image. Pixels above the threshold are assumed to be examples of the gas and will be averaged to provide the signal statistics. Similarly, pixels below the threshold will represent the background and will be averaged to calculate the background average and the background covariance matrix needed in Equation 1.
The determination of the threshold to separate between the background and the signal will be determined by the statistics of the background. For the rest of this paper, the threshold for the gas was calculated as that being two standard deviations about the mean of the background.

c. Experimental Results:

The initial image shows the results from the correlation coefficient (Fig. 10). The matched filter results can be seen in the next image. The statistics of the background can be seen in the third image, while the new estimate of the location of the gas pixels is in the fourth image.

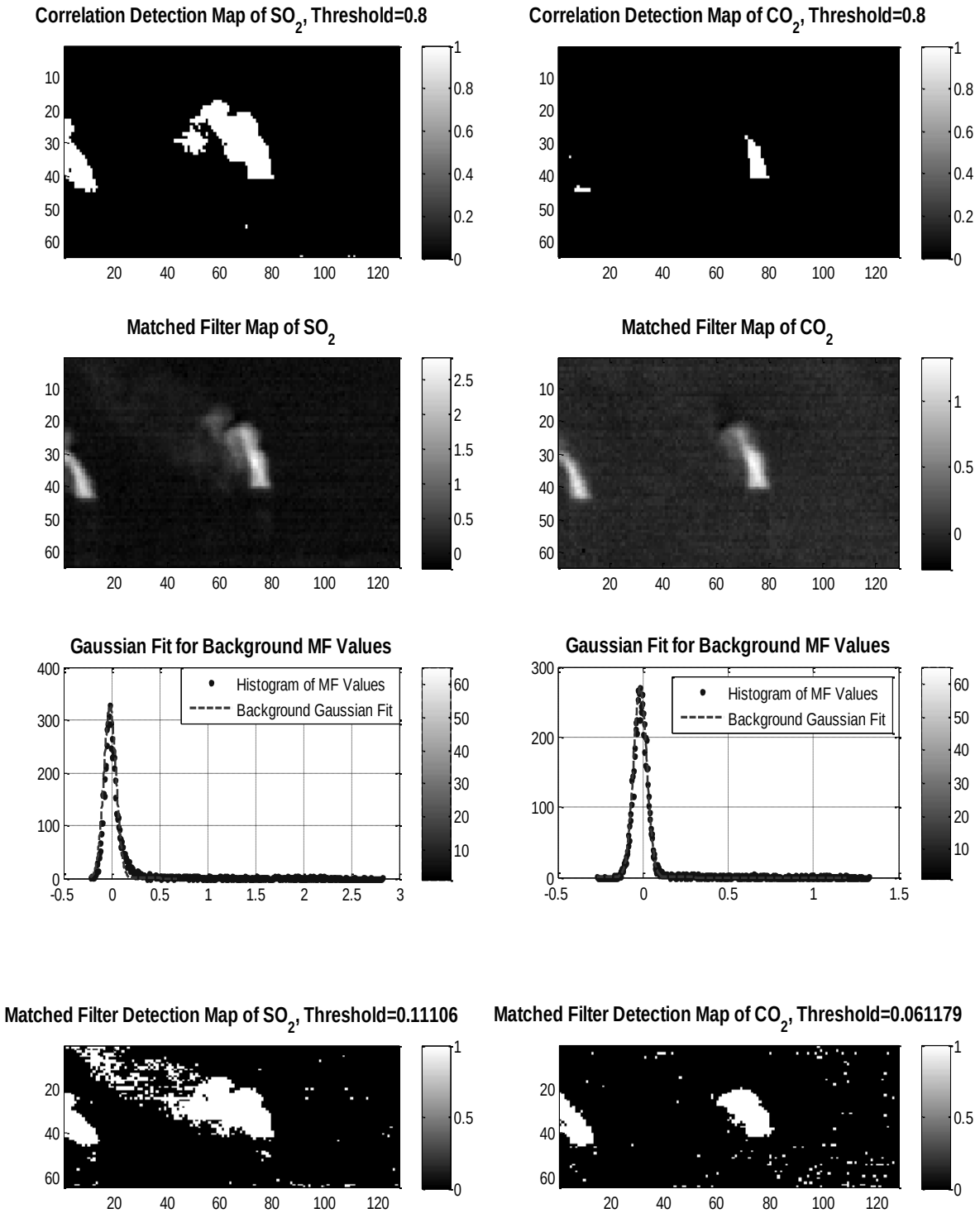

Fig. 10: CO_2 and SO_2 gas pixels: a) initial estimate based on correlation coefficient, b) matched filter result, c) histogram of matched filter result and d) new estimate of gas pixel location

We note that the concept of using the actual data iteratively to find the actual signature of the data for the next analysis is critical. In the next figure (Fig. 11), we show what one obtains if one had continued to use the laboratory signal without using the actual data (thereby ignoring atmospheric and sensor effects).

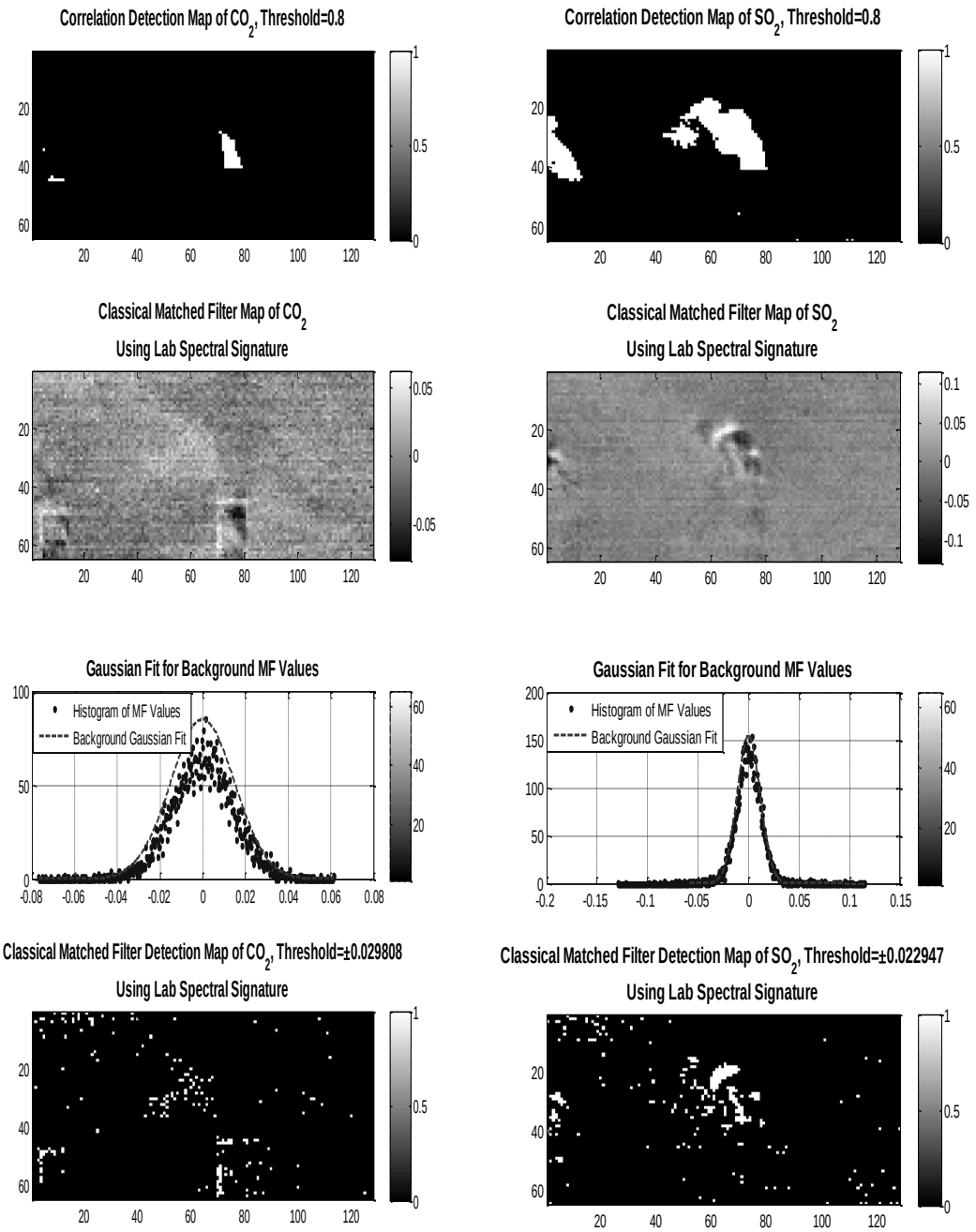

Figs. 11: Same data as in Fig. 10 with the exception that CO_2 and SO_2 library signals were used to model the expected gas signature, rather than the experimental data.

The results in Fig. 11, in particular for CO_2, seem to be particularly poor.

Our method when applied iteratively several times seems to converge on a particularly good result (Fig. 12).

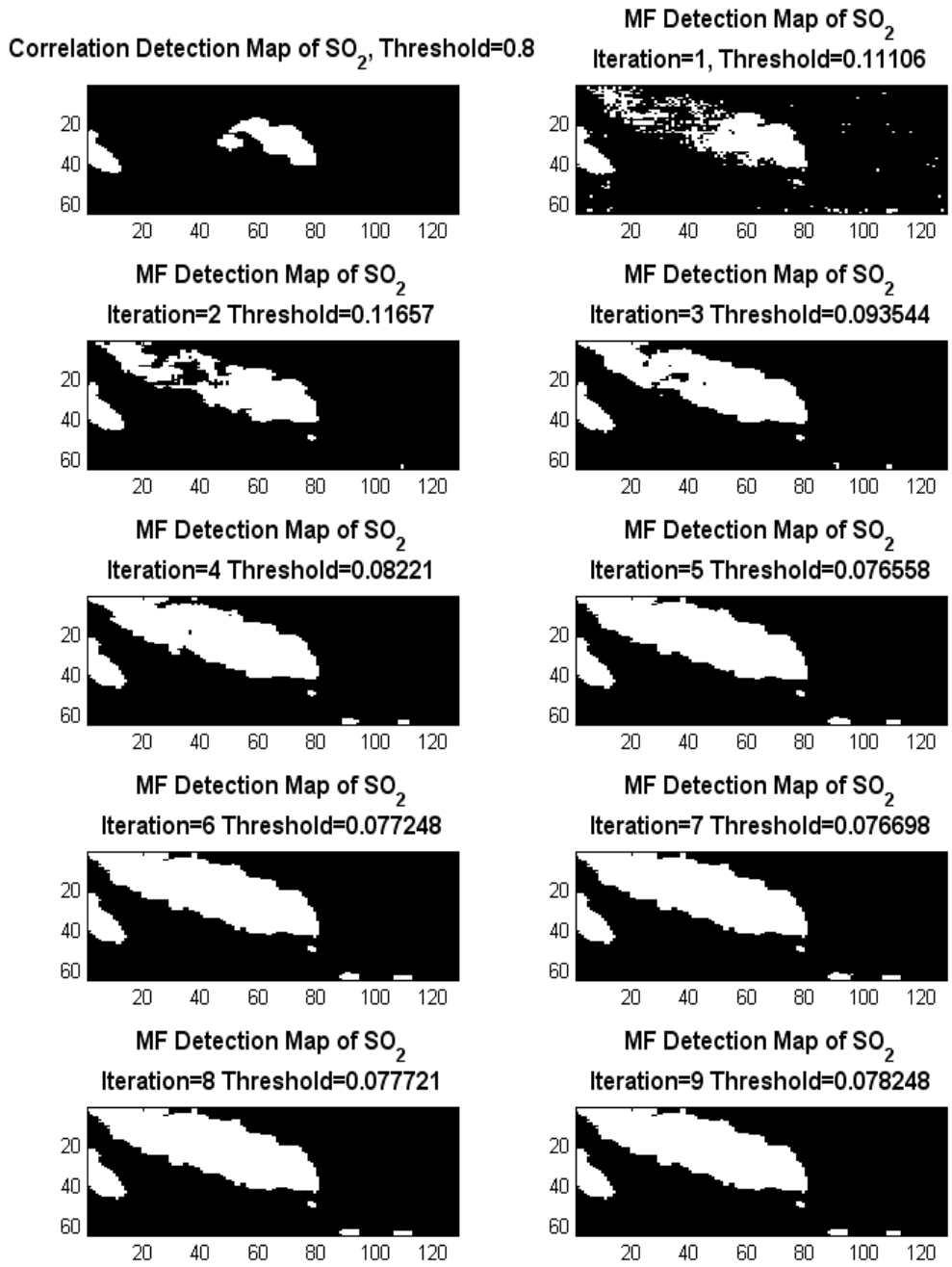

Fig. 12. Convergence of our method after 9 iterations for the detection of SO_2.

For the sake of completeness, the original images and the final results for CO_2 and SO_2 for 400 and 1700 meters are shown in Figs. 13-16.

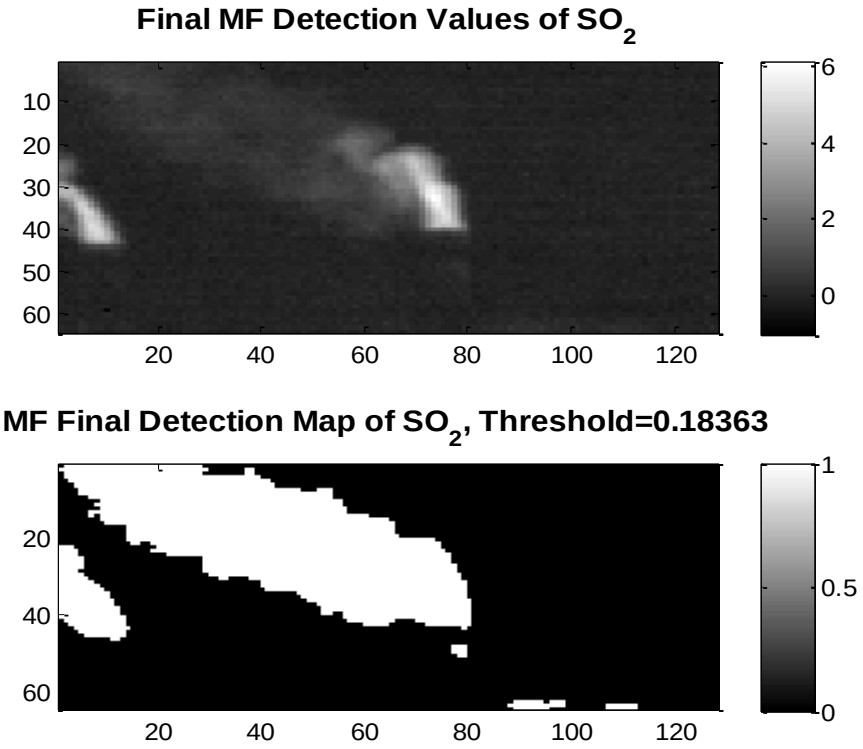

Fig. 13: SO_2 - 400 meters

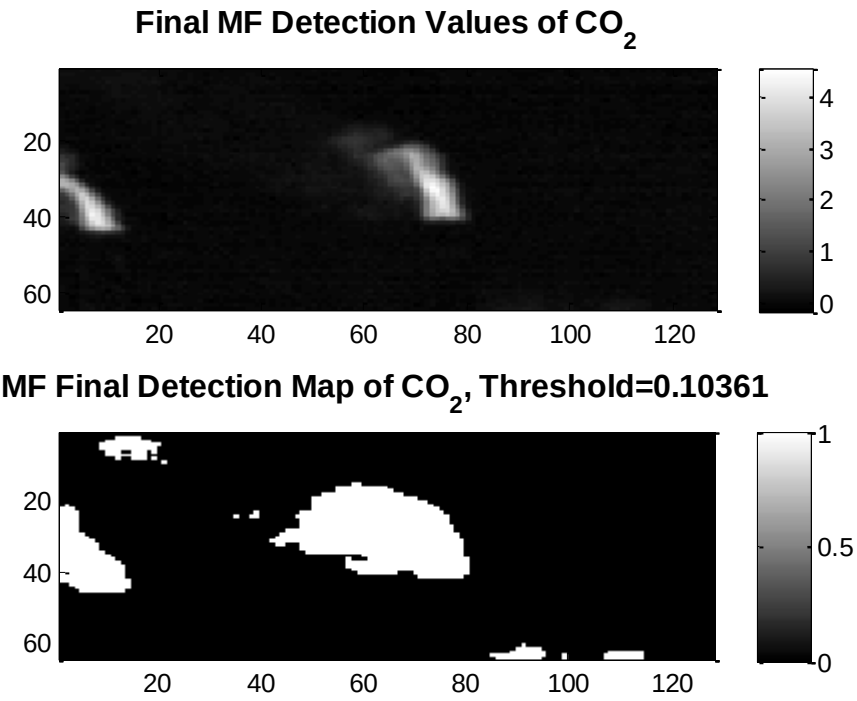

Fig. 14: CO_2 – 400 meters

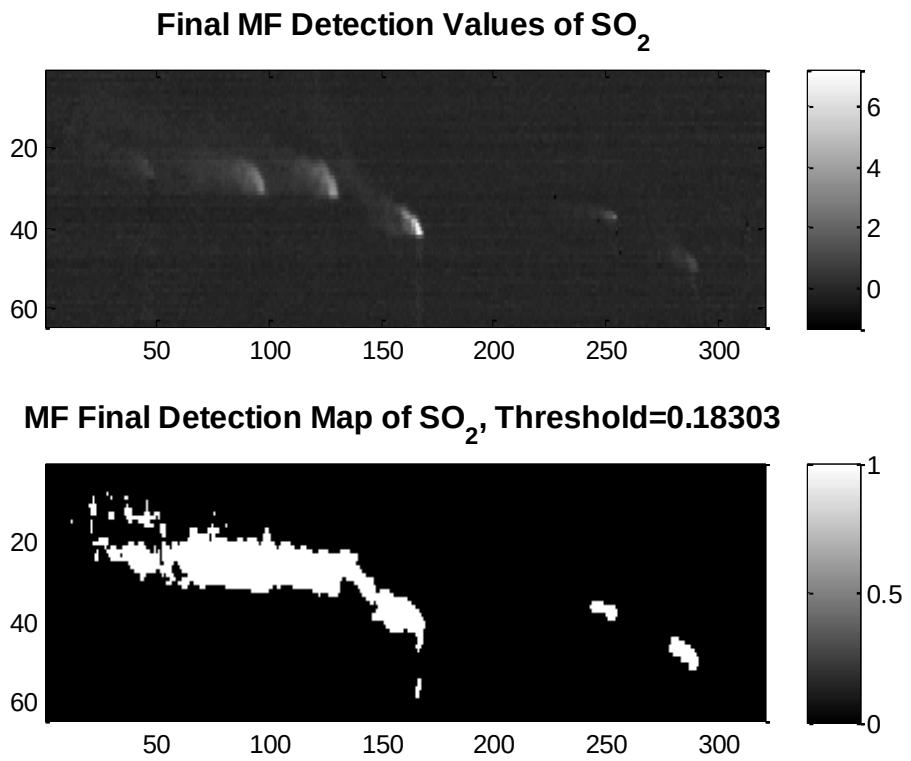

Fig. 15: SO_2 – 400 meters

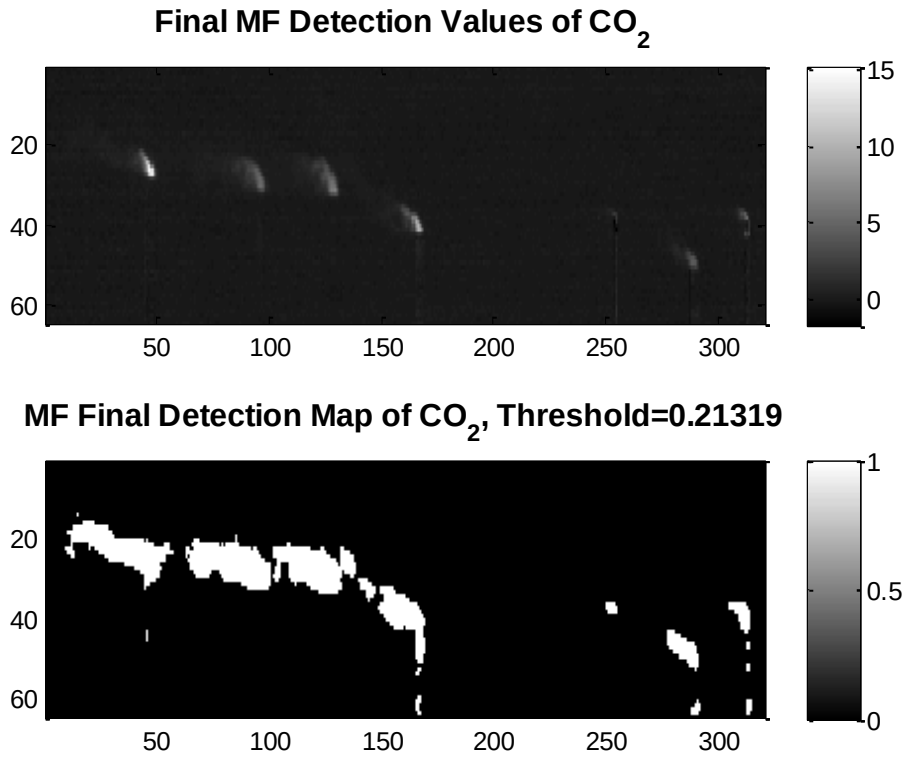

Fig. 16 – CO_2 - 1700 meters.

IV. Proportional Concentrations of Gases:

Now that we have identified the gases present and their extent, it is interesting to consider their relative concentrations. In order to do this calculation, we must assume that the temperature difference between the background and the gas is spatially a constant; in this section we make such an assumption. Thus, the primary difference in the spectra is due to different concentration. In Section V, we will consider how to use the temperature dependence of the gas absorption to separate the two effects (concentration and temperature) one from the other

Let us consider a pixel which consists of the gas at a certain temperature and concentration with the background of the sky. Since the sky in the infrared will be much colder than the gas, we can assume that the signature received will be the signature of the sky plus a component due to the gas.

We can calculate the ratio of the power due to the two gases compared to the power due to the background. This would be done as follows:

Let M be a matrix whose columns consist of the laboratory signatures of the gases.

$$\mathbf{M} = \begin{pmatrix} \vdots & \vdots & \vdots \\ \vec{s}_1 & \cdots & \vec{s}_N \\ \vdots & \vdots & \vdots \end{pmatrix} \qquad (2)$$

Each pixel can now be projected into this subspace via Equation 3:

$$\vec{\alpha} = \left(\mathbf{M}^T\mathbf{M}\right)^{-1}\mathbf{M}^T\vec{r} \qquad (3)$$

The vector alpha represents the fractions of the gas vectors (in M) which have been found. The vector in this subspace can be decomposed into the specific gas signatures representing the gases by Malpha; the component of the original vector orthogonal to this space is related to the background and the noise. Two interesting parameters can now be determined for each pixel: the first is the coefficients of each of the gases, the second is the ratio of the power of the combined gas signatures to the original pixel. The fit we showed in Fig.4 was obtained by this method.

The ratios of the power of the gases to the overall power of the pixels is shown in Figs. 17 and 18 for 400 and 1700 meters, respectively.

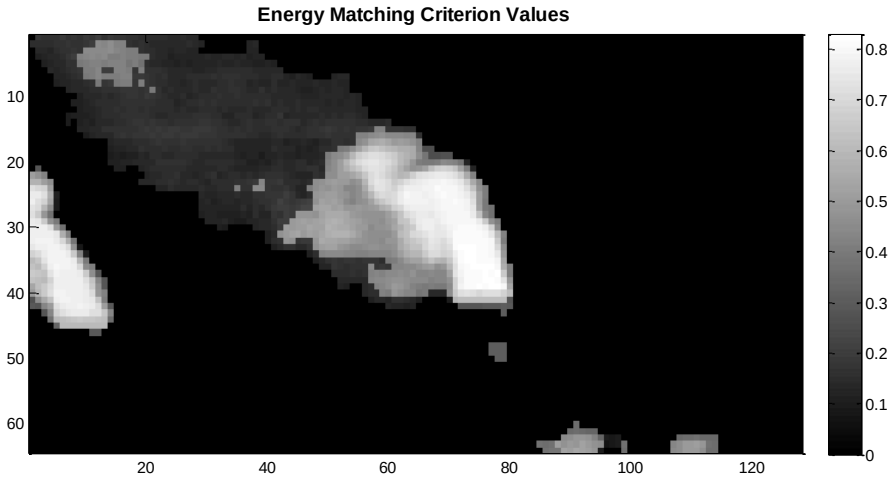

Fig.17: Energy ratio of the power associated with the two gases to the overall power for 400 meters

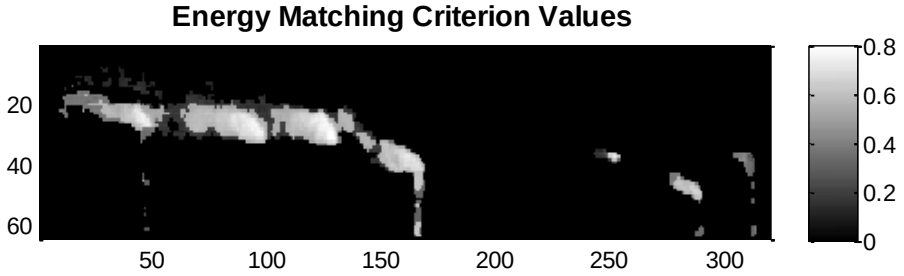

Fig. 18: Energy ratio of the power associated with the two gases to the overall power for 400 meters.

The actual coefficients for CO_2 and SO_2 for 400 and 1700 meter range can be seen in Figs. 19-22.

.

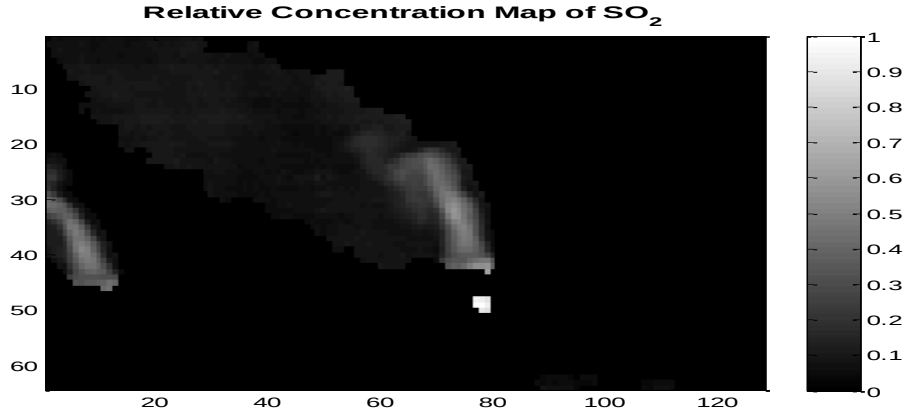

Fig. 19: SO_2 - 400 meters.

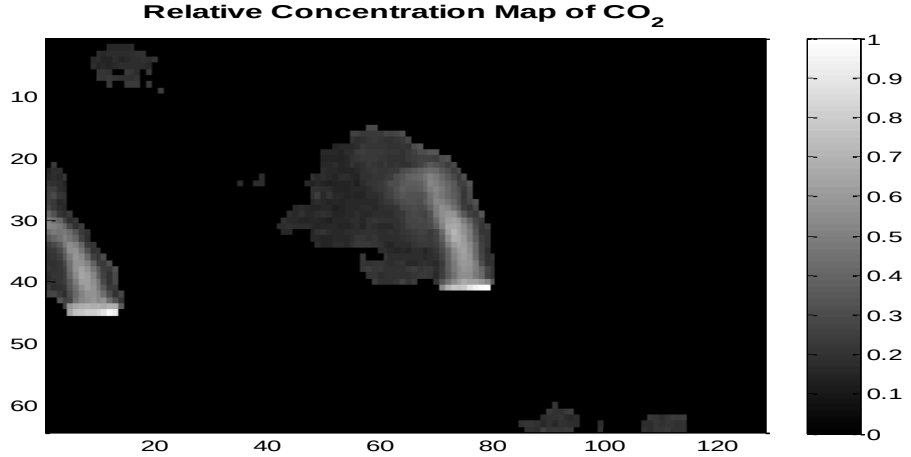

Fig. 20: CO_2 – 400 meters

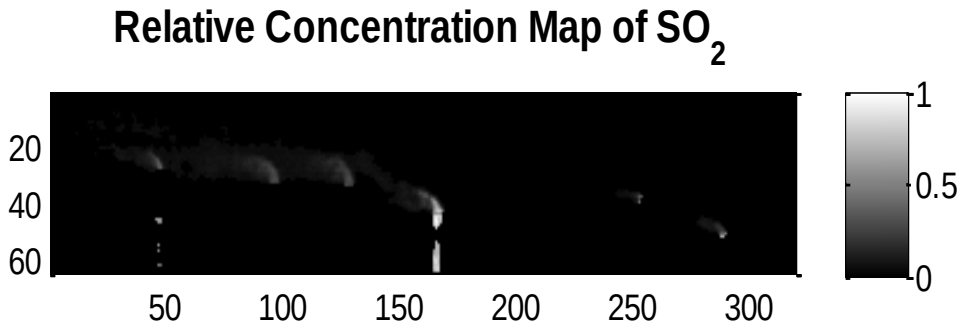

Fig. 21: SO_2 – 1700 meters

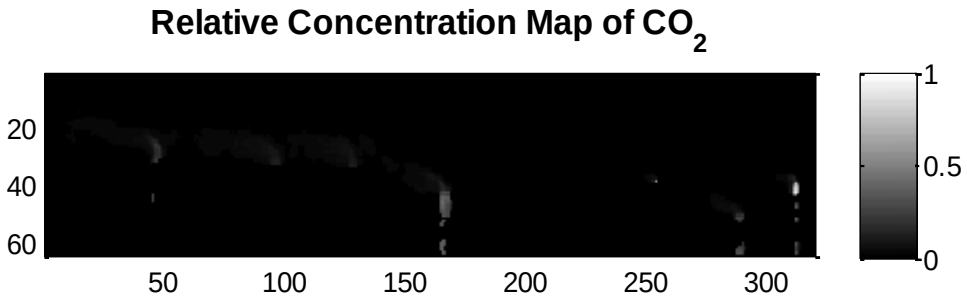

Fig. 22: CO_2 – 1700 meters.

V. Quantifying concentration and temperature separately:\

a. Method

It is known that the observed signature will be a function of the product of the concentration and the temperature. In other words, assuming a linear form of Beer's law, a doubling of the concentration will produce the same resultant spectral signature as a doubling of the plume temperature.

To avoid this problem, we note the following: the temperature observed at any pixel, corresponding to a particular physical location, is the same for all the chemical species located there. However, very often the temperature dependence of one of the gases chemical absorption can be very different from other species' temperature dependencies. Under certain assumptions, we can invert for the temperature.

We will assume that in our gases the temperature dependence of the SO_2 and CO_2 transitions are known. The steps necessary to then derive the temperature are as follows:

1. Take the pixel signature and normalize it:
    i. One must remove the background signature. This in general can be done by defining the background as a typical non-gaseous sky pixel and subtracting it from the inspected pixel.
    ii. One should remove any residual DC effects by finding the wavelength which in general has the lowest value (and thus is most likely to be unaffected by the gas) and subtracting its value from all the other wavelengths.
    iii. One should find one of the predetermined wavelength peaks of the signal and divide all the values in the signal by it. When this is performed on all the pixels, the pixels will now be normalized with zero at the lowest wavelength and one at one of the highest peaks.

Let us assume that the gases do not separate in the atmosphere; in other words, the ratio of the two concentration of the two gases is constant in all pixels. In that case, since we have normalized the curves, the effect of different concentrations has been eliminated. Therefore,

2. Measure the ratio of the two species.
    a. This can actually be done in several ways. One can simply pick the peak values of each of the two species and take the ratio. Alternatively, one can integrate over some range of wavelengths for each of the species and take the ratio of these values.

If the temperature dependence of each species was identical, the signatures would be identical (within the limits of the noise) and the ratios would be constant. Changes in the ratios must be due to the different temperatures at which each pixel finds itself and the chemical response to these differences.

3. Assume a temperature for some particular pixel.
    a. Although we can see the change in the above metric, we do not know what the actual concentration ratio of the two gases is. Thus, one peak may be much larger than the second either because the ratio of the gases is much larger or because the temperature is much more appropriate for one gas relative to the second. Some physical estimate of the temperature of at least one pixel must be made.

4. Calculate the temperatures for the remaining pixels
    a. The temperature of the remaining pixels can now be calculated relative to the value assumed for the first "known" pixel in Step 3.

5. Calculate concentrations.
    a. Given the temperature at each point, we can calculate the relative concentration spatially of each gas component. Due to the assumptions preceding Step 2, the distributions will be identical.
    b. Note that if the absolute strength of the transitions are known and if the spatial extent of the gas in the third dimension perpendicular to the plane of the image is known, then absolute concentrations can be calculated.

b. **Experimental Results**:

In Figs. 2 and 3 in the beginning of the paper, we presented the laboratory absorption spectra for CO_2 and SO_2 respectively, as a function of temperature and wavelength for constant concentration (EPA data is given at http://www.epa.gov/ttn/emc/ftir/aedcdat1.html). The SO_2 spectra noticeably decrease as a function of increasing temperature, while the CO_2 spectra correlate positively with increasing temperature.

The situation we postulated in the previous sections exists; there is a dramatic temperature difference in behavior for the absorption between two of the gaseous components in the gas.

After normalizing the peaks to eliminate concentration effects, as described above, we must choose a feature which has a strong temperature dependence. We will base ourselves on the ratio of the first SO_2 peak at roughly 8.5 micron to the second CO_2 peak at 9.7 micron.

The temperature dependence of these peaks based on the laboratory measurements can be seen in Fig. 23

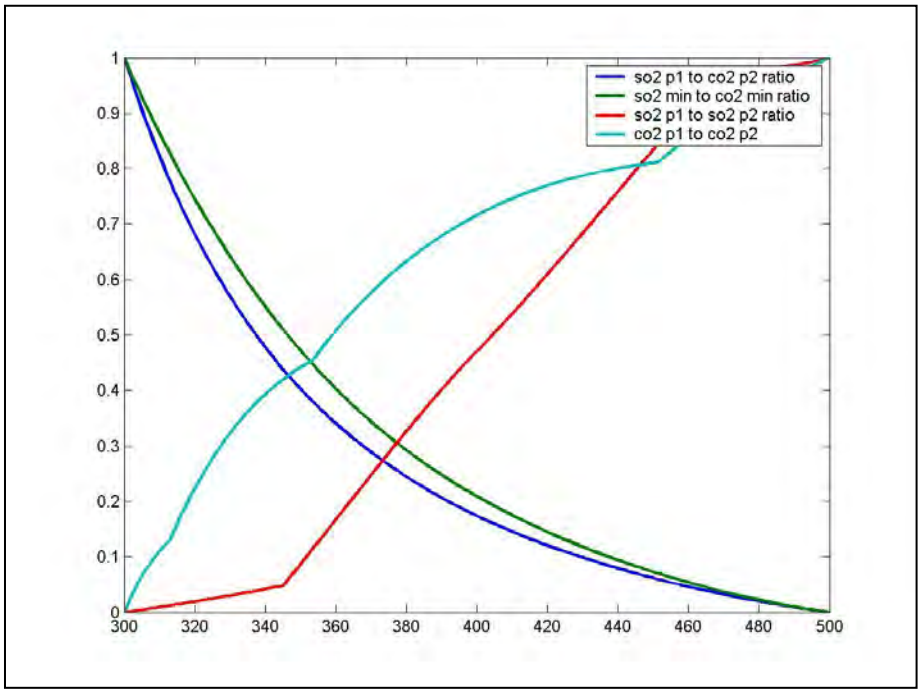

Fig. 23: Ratio of peaks after normalization (the first two at 300 degrees, the last two at 500 degrees), as a function of temperature.

The pixel with the highest temperature-concentration product in Fig. 17 was assigned the temperature of 500 degrees and was the basis for our normalization. Fig. 24 shows three pixels which have been normalized as discussed above. The prominent SO_2 peaks at the coldest temperatures on the left of the graph and the CO_2 peaks at the right of the graph, notable at high temperatures, can be seen.

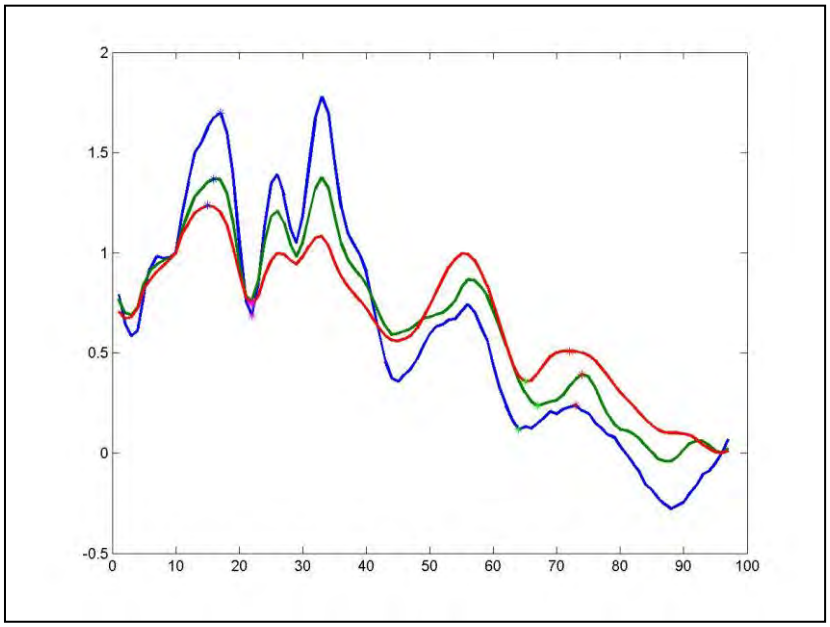

Fig. 24: Note that the blue curve represents a pixel far from the stack, the red curve is close to the stack and the green curve is intermediate between the two. Normalization occurs at bands 8 and 95.

Fig. 25 shows the temperature prediction results on the pixels associated with the gas emission. The overall success of the method can be seen by the consistency of the data. Although we have normalized the data at two bands, the shape and intensity of the peaks allows us to determine the temperature. Note that the temperature appears to be hottest slightly above the stack; it gets consistently cooler as we go downwind.

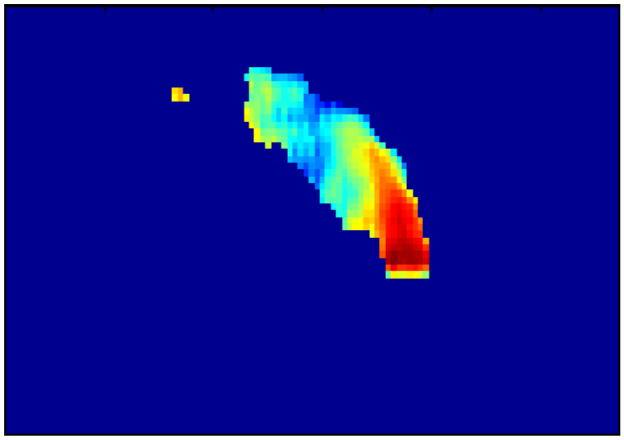

Fig. 25: Temperature distribution for the gas cloud.

Fig. 26a:

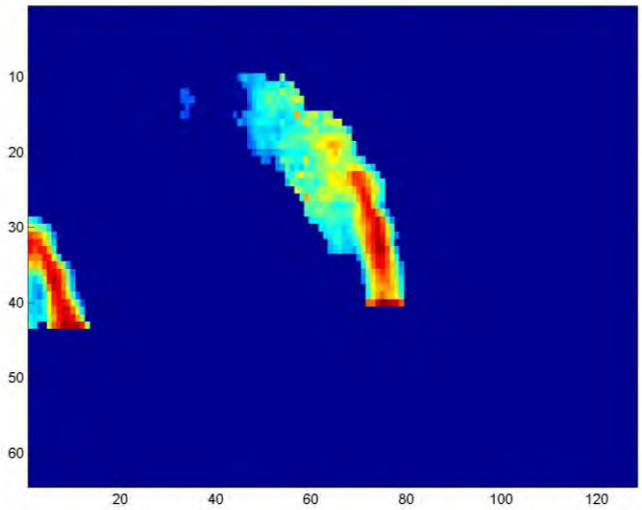

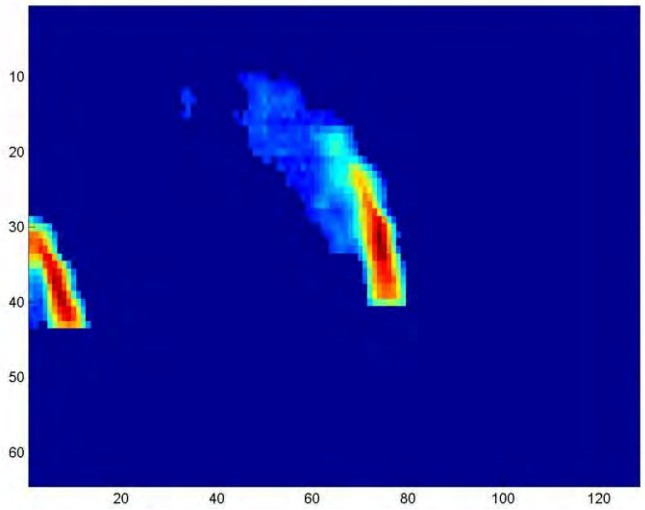

Fig. 26b:

Figs. 26 a and b: Concentration maps for a) CO_2 and b) SO_2.

Fig. 26 shows the gas spatial distribution once the temperature has been accounted for. It shows similarities to the temperature distribution as would be expected: as the gas flows away from the stack it decreases both in temperature and concentration. Nevertheless, there are some subtle differences. The highest concentration is not immediately above the stack, but rather a slight distance above it. This can be noted in previously published theoretical models (Halitsky, 1968). (Figs. 27 and 28).

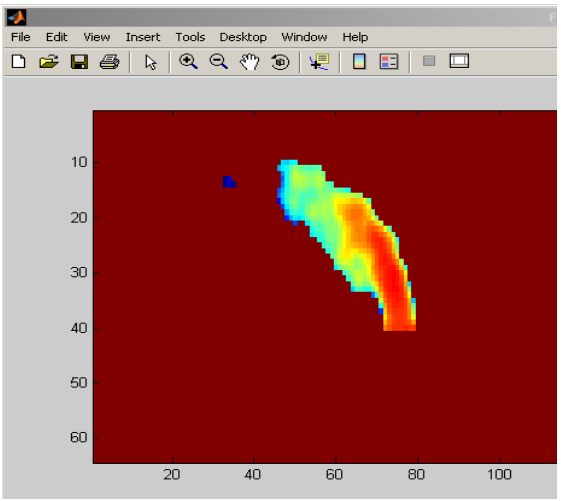

Fig. 27: Theoretical gas temperature distribution. [Halitsky, 1968]

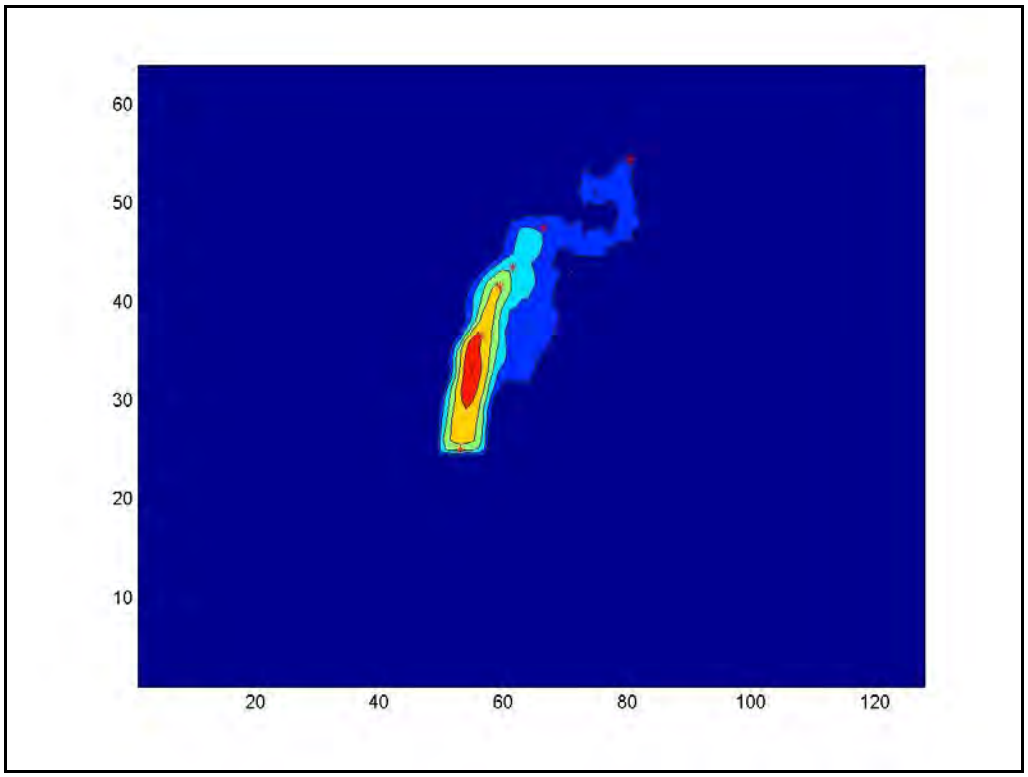

Fig. 28 Theoretical gas distribution [Halitsky, 1968].

VI. Conclusions

The research here has been divided into three parts. We started with gases being emitted from a smokestack. Not knowing what gasses were being emitted, we developed a method to correlate known laboratory spectra with the emitted spectra. We found the two main components: carbon dioxide and sulfur dioxide. Our method for doing this involved the careful selection of critical wavelengths for the analysis.

While this enabled us to find the main concentrations of gas, we wanted to extend the physical extent of the cloud. We did this by shifting from the laboratory signatures to the actual averaged real data signatures of the gas cloud and then performing a matched filter. The image was then thresholded on the basis of the background statistics. This procedure was performed iteratively until a stable division of background/gas was achieved.

The resulting signatures can be separated by energy into that which is due to the gases and that which due to the background; the percentages of each gas can be calculated. Finally, we successfully separated the temperature from the gas by recognizing the different temperature dependences of the gas components.

References

Shaw, G.A., & Burke, H.K. (2003). Spectral Imaging for Remote sensing. *Lincoln Laboratory Journal*, 14, 3-28.

Czerwinski, R.N., Farrar, K.E., Griffin, M.K., & Kerekes, J.P. (2005). Spectral Quality Requirements for Effluent Quantification. *SPIE*, 5425, 616-627.

Farley, V., Vallieresa, A., Chamberlanda, M., & Villemaire, A. (2006). Performance of the FIRST, a Longwave Infrared Hyperspectral Imaging Sensor. *SPIE*, 6398, 63980T.

Kopeika, N.S. (1998). A System Engineering Approach to Imaging. *SPIE*.

Manolakis, D., & Shaw, G. (2002). Detection Algorithms for Hyperspectral Imaging Application. *IEEE Signal Processing Magazine*, 19, 29-43.

Figov, Z., Wolowelsky, K., & Goldberg, N. (2007). Co-registration of hyperspectral bands. *SPIE*, 6748, 67480S.

Theiler, J., Foy, B.R., & Fraser, A.M. (2006). Nonlinear signal contamination effects for gaseous plume detection in hyperspectral imagery. *SPIE*, 6233, 62331U.

Douet, J. (1988). *Going up in Smoke:The History of the Industrial Chimney*. Victorian Society, London, England. Victorian Society Casework Reports.

EPA data given at http://www.epa.gov/ttn/emc/ftir/aedcdat1.html.

James A. Halitsky (1968). "Temperatures and concentrations in heated plumes". Atmospheric Environment **2(4),** 419-422.

Gas detection from smoke stacks: finding multiple constituent gases in a plume using infrared hyperspectral data

D.N. Rotman[1], S.R. Rotman*[2,3], D. G. Blumberg[2], E. Ontiveros[3], and D. Messinger[3]
[1] Dept. of Electrical Engineering, Technion-Israel Institute of Technology, Technion City, Haifa
[2]Department of Electrical and Computer Engineering and The Earth and Planetary Image Facility, Ben-Gurion University of the Negev, P.O.B. 653, Beer-Sheva 84105, Israel
[3]Center for Imaging Sciences, Rochester Institute of Technology, Lomb Memorial Drive,Rochester, NY USA 14623-5603

ABSTRACT

An iterative algorithm which identifies the presence of different gases using a hyperspectral image was developed and tested. The algorithm uses the "stepwise regression" method combined with new methods of detection and identification. This algorithm begins with a library of gas signatures; an initial fit is done with all the gases. The algorithm then eliminates those signatures which do not noticeably improve the fit to the measured signature. We then consider which of the gases that were detected have a high probability of being mistaken with the detection of other gases that are also present in the scene. A necessary post-processing step eliminates gases which do not uniquely fit the signature of the examined pixel, with an emphasis on eliminating gases which may have been misidentified.

Keywords: gas detection, stepwise regression, longwave infrared

1. INTRODUCTION

Hyperspectral image processing is based on the fact that each material has its own unique "spectral signature". In general, any pixel of a hyperspectral image will consist of a mix of hyperspectral signatures. Linear unmixing techniques are designed to separate these pixels into their constituents.

This procedure is even more complicated when applied to gas detection. In any one pixel of an image of a gas plume, we may expect to see the emission (or absorption) signatures of several gases, background behind the plume emission, and atmospheric absorption. Thus, the unmixing will have a particularly complicated algorithm to properly identify and quantify the gases present. [1]

The spectral signatures of many gases have absorption and emission lines in the LWIR (Long Wave InfraRed) and MWIR (Medium Wave InfraRed) spectral regions, i.e., 8-12[μm] and 3-5[μm], which enable gas detection in the analysis of hyperspectral cubes containing those wavelengths. Due to the increasing need in means to monitor industrial polluting, a method of quickly and efficiently detecting gases which are emitted into the atmosphere by industrial plants is useful. [2]

In this paper, we develop a stepwise regression method to detect gases in a plume; our initial report of the method may be found in Ref. 3. We augment this previous report with a new method for the detection of multiple gases which takes into account that gases may often be mistaken one for another. Therefore, after our initial phase in which we determine which gases are apparently present, we examine the pairs of gases present, considering which gas could have been confused as another. The threshold for positive detection is raised depending on how similar two gases are.

*srotman@ee.bgu.ac.il; phone +972 8 646-1539; fax +972 8 647-2949

2. ALGORITHM DEVELOPMENT

2.1 The implementation of the stepwise regression method. [1],[3]

A regression approach for gas identification, called stepwise regression, was suggested in Ref. [1]. Our implementation is described as follows:

Each pixel can be described as

$$\vec{p} = \overrightarrow{\overrightarrow{M}\vec{\beta}} + \vec{n} \quad (1)$$

where p is the pixel's values throughout the different wavelengths, M is a matrix containing the signatures of all the gases potentially present in p, $\vec{\beta}$ is the gases

signature's abundances, and n represent noise and clutter, i.e., signatures which are present in the pixel and aren't a known gas.

The stepwise regression algorithm receives a matrix M which contains the signatures of all the gases to be checked for their presence. It then calculates $\vec{\alpha}$ which is an estimation of $\vec{\beta}$:

$$\vec{\alpha} = \left(\vec{\vec{M}}^T \vec{\vec{M}}\right)^{-1} \vec{\vec{M}}^T \vec{p} \approx \vec{\beta} \quad (2)$$

The algorithm next removes sequentially each of the gas signatures from M and calculates the corresponding $\vec{\alpha}$ and the "fit error test" E.

$$E = \frac{\vec{p}^{-1}\vec{p} - \vec{\alpha}^{-1}\vec{\vec{M}}^{-1}\vec{p}}{N - R} \quad (3)$$

N is the number of channels in the cube and R is the number of gases which are in the databank but have been removed and are not being used in M. The "fit error test" is the average energy (per channel) of the difference between the revaluated pixel and the actual pixel, with a slight penalty for removing the gases from M. The algorithm then returns the previously removed gas to M and proceeds to the next one.

After processing all the gases, the algorithm compares all new "fit error tests" caused by removing each of the gases to each other and removes permanently the gas whose removal has the smallest effect on the "fit error test" This assumes that the relative rise in the error is less than a given threshold (0.15 in this experiment).

2.2 Shift fitting method

Upon examination and comparison of the spectrum of a certain pixel and a particular gas, it is often possible for a human to immediately see whether the gas is present or not, by comparing the local maximum and minimum points of the two vectors. A method of imitating this process is described below. For each gas a "signature's highlights" vector is created. This is a vector containing only the local maxima and minima points of the signature minus the total average of those points. The rest of the channels contain zero values. The average of those "signature's highlights" is 0.

A "picks fit" value for each pixel-gas combination is calculated as:

$$pick_{fit} = \vec{p}^T \vec{h} \quad (4)$$

Where h is the "signature's highlights" vector of the investigated gas. Originally, the wavelengths of the gas vector are aligned with the wavelengths of the investigated pixel (as is logical). We next shift the "signature's highlights" vector circularly one channel at a time. For each shift a new "picks fit" is calculated, producing a vector $\vec{S}$, representing the "picks fit" values for the different shifts. The larger the "picks fit"

value at 0 in comparison to the rest of the shifts, the more likely the tested gas is present. To quantify this, a new metric presence likelihood test ("PLT") is calculated:

$$"PLT" = \frac{\vec{s}[0] - mean(\vec{s})}{std(\vec{s})} \quad (5)$$

where std is the standard deviation. The algorithm uses this test for all of the pixels and for each of the gases tested and chooses the gases where PLT1>1.4 as present. The algorithm then applies another technique based on the same principle, using the stepwise regression's results. It repeats the exact same process as the method described above, with one difference: Instead of using the pixel's spectrum vector, it uses a vector $\vec{X}$ which is the fit error (produced by the stepwise regression)+tested gas component in the fit:

$$\vec{X} = \left(\vec{P} - \vec{\vec{M}}\vec{\alpha}\right) + \alpha[j]\vec{M}[:, j] \quad (6)$$

where j is the index of the tested gas.

This method is meant to magnify the effect of the presence/non presence of the tested gas and eliminate effects of other gases maximum and minimum points in the pixel. The algorithm uses this test for all of the pixels, but only for the gases which were identified by the stepwise regression step in each pixel. It identifies as present the gases where PLT2>0.65. After applying both of these methods, it combines their results (a simple AND operator).

3. INITIAL RESULTS

3.1 First Data-Set

Initially, the above algorithm was applied to a natural scene: The algorithm was tested on a hyperspectral cube taken by a TELOP "F.I.R.S.T" camera. The picture was acquired from the chimneys of Haifa's refineries facilities. The cube contains 225 channels in wavelengths from 7.5μ*m* to 12μ*m*. According to the factory's published data, CO2 and SO2 are emitted in high quantity. Figure 1 shows an optical and infrared (shown in false color) image of the scene.

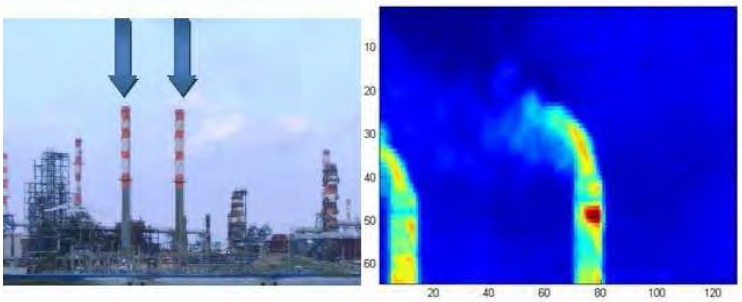

Figure 1. On left, Haifa chimneys. On right, close-up of images

The algorithm was activated with a signatures bank of 11 gases: BENZENE, CH4, CO_2, F12, F114, H_2O, N_2O, NH_3, O_3, SO_2, NO_2. Their spectra can be seen in Figure 2.

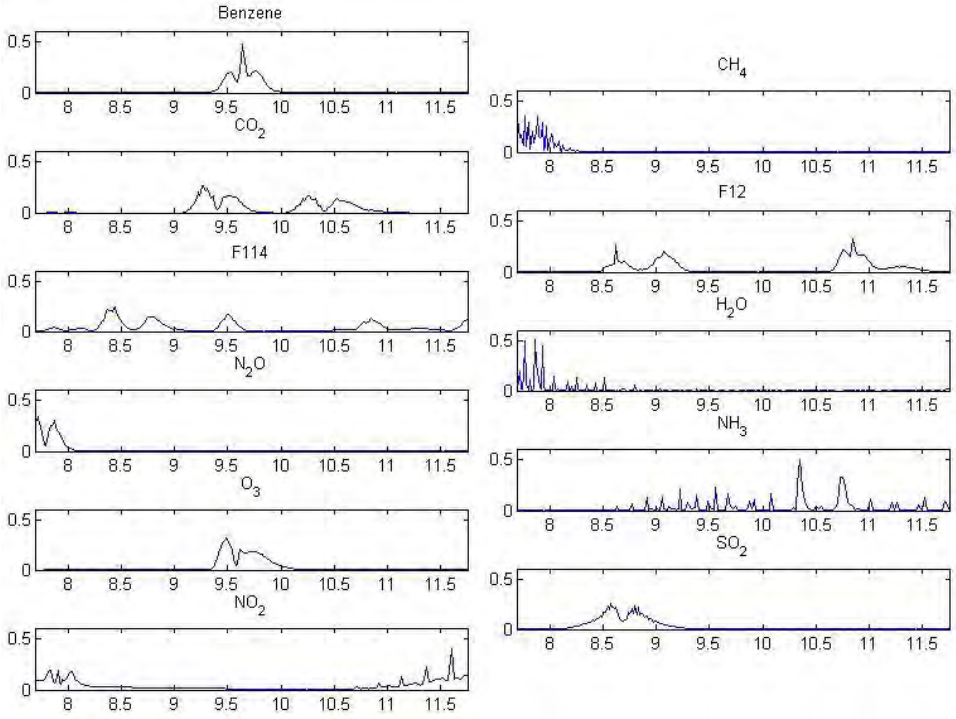

Figure 2. Gas spectra library

When looking at the spectra of a pixel taken from the center of the gas emitted from the stack, the "human eye" can recognize the presence of CO_2, O_3 and SO_2 gases immediately, as seen in Figure 3. (The ozone may be seen either in the plume or in the background atmosphere; throughout this paper, we will consider ozone to be neither a detection or a false alarm).

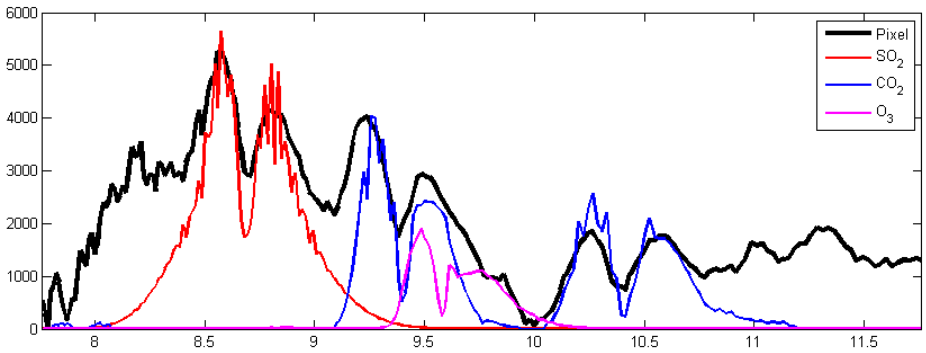

Figure 3. Pixel spectra and gases easily identified

The basic algorithm as described in Section II.1 produces a large number of false alarms. The results can be seen in Figure 4.

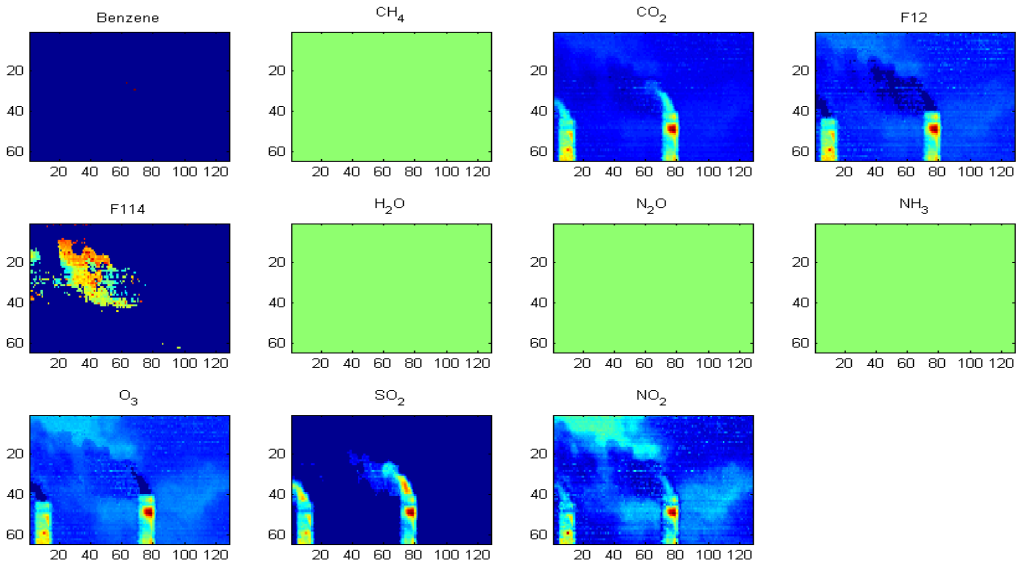

Figure 4. Initial results: gases detected after running stepwise regression

After we run the shift algorithm, most of the false detections are removed including the detection of gases in the stack, as seen in Figure 5.

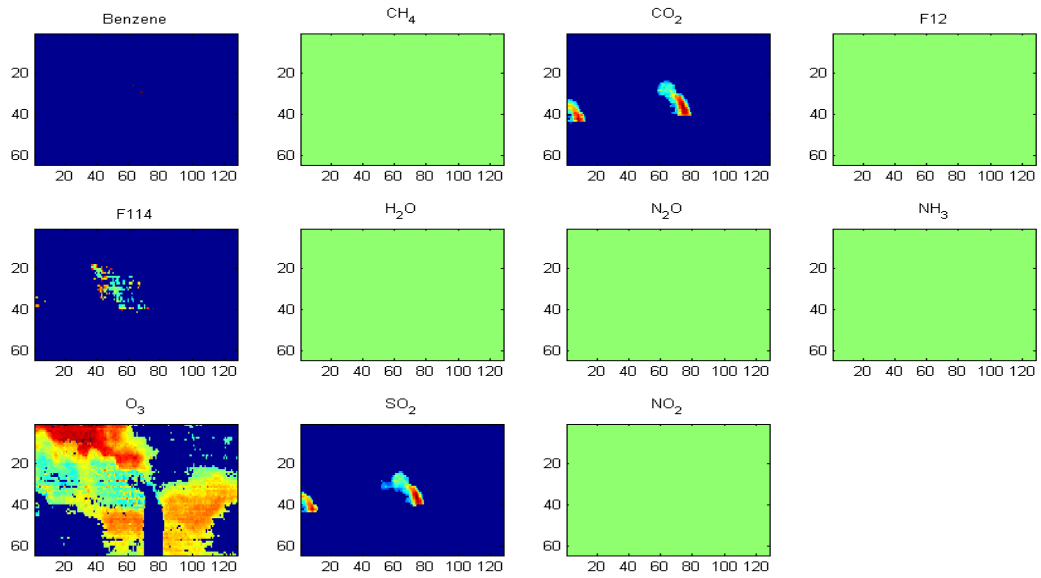

Figure 5. Gasses detected after shift algorithm was applied Note that Benzene has a few false detections.

As we can see, the algorithm was considerably improved. In the gas cloud, we detect SO_2 and CO_2, while O_3 is detected in the atmosphere. Trace amounts of F114 and Benzene were found; from their spatial distributions, we believe that these detections are false alarms.

The PLT thresholds previously mentioned in Section II.2 of PLT1>1.4 and PLT2>0.65 were reached by trial and error; these were the best results that could be obtained, and the problem of the false alarms of F114 and Benzene was at this stage unsolvable. We will show that after the new post-processing step we implemented, these false alarms are fixed.

3.2 Second Data-Set

We continue by applying the above algorithm to a DIRSIG image [1]. The particular image we chose was a horizontal image with a gas plume clearly visible (Fig. 6). This image is shown in false color as imaged at 9 microns. The plume itself consists of SO_2 gas; a standard atmosphere was assumed.

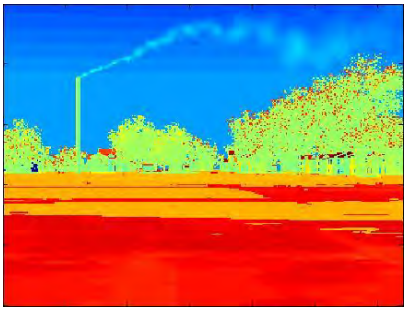

Figure 6a. DIRSIG Image in false color plotted at 9

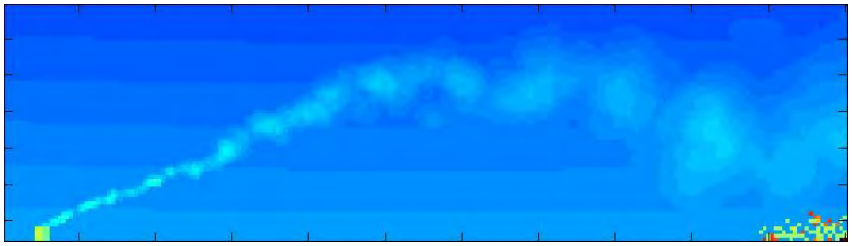

Figure 6b. Area of interest

With the same gas signature bank as before, we can see again that the basic algorithm described in Section 2 produces a large number of false alarms (Fig. 7).

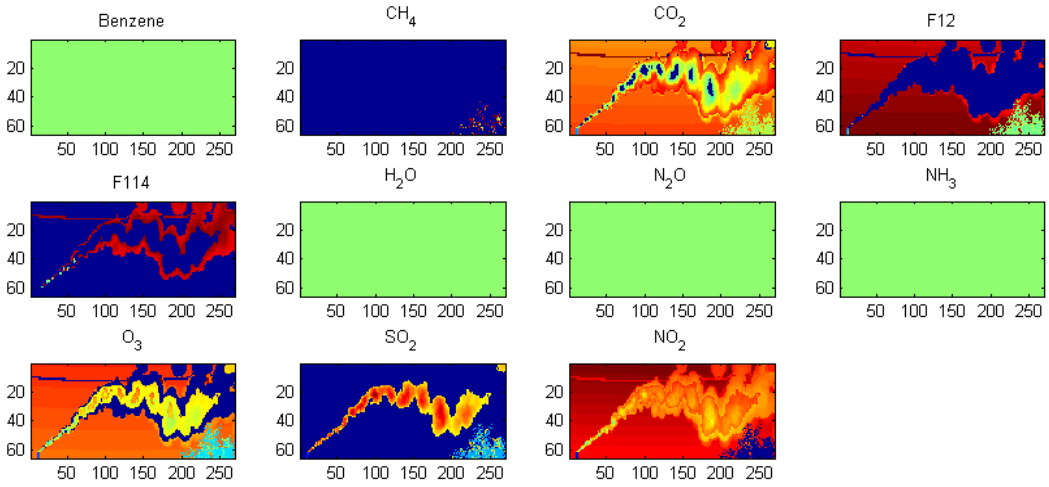

Figure 7. Initial results after applying shift algorithm

When trying to implement the shift algorithm we encountered the following problem: there were no PLT1 or PLT2 values which could be chosen which would leave the SO_2 gas in and yet eliminate all the others. The best results which could be reached are shown in Figure 8.

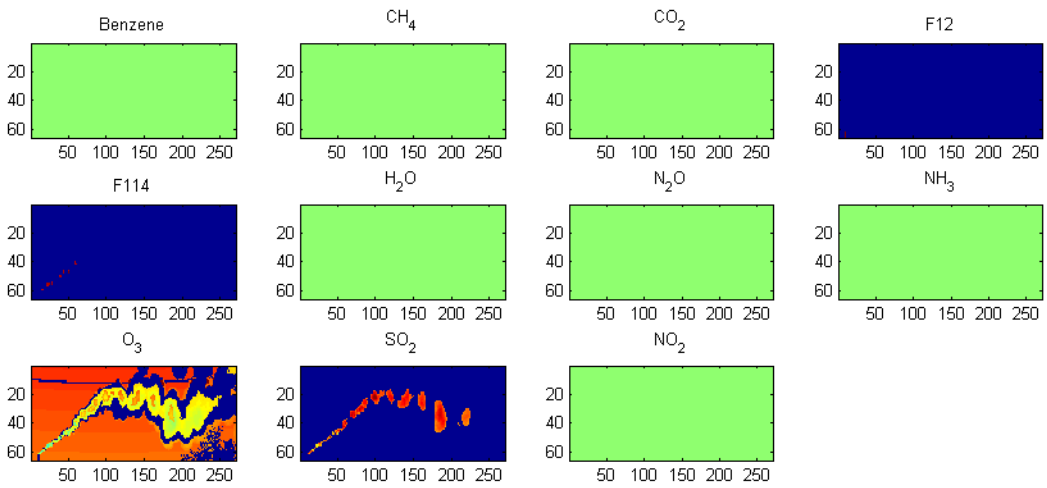

Figure 8. Initial results: DIRSIG data after running stepwise regression

We are left with some false alarms. F114 is detected where the gas cloud is strongest, and F12 is being detected in a few pixels in the stack.

We noted that the PLT values derived were sometimes much higher for some gases compared to others. Apparently, what we need is not an absolute PLT score, but a relative gas-dependent threshold. In addition, some gases can be mistaken as other gases if their spectra are similar.

In order to eliminate these false detections we developed the following algorithm presented in Section 4.

4. COMPARING SIMILAR GASES

One of the problems which we may have is that many gases are similar to one another. Therefore, it behooves us to consider how we can avoid having gases interfere with one another.

Let us consider the results of shift when one "pure" gas is run against another pure gas. The shift algorithm was run on a "cube" which consisted of 11 pixels – the pixels being the gas signatures themselves. The row is the gas which the pixel looks like; the column is the gas which we are trying to detect in the pixel. We include the case where a gas is run against itself. The shift results are shown in Table 1.

Table 1. The shift results received when comparing gas spectra.

gas / pixel	Benzene	CH4	CO2	F12	F114	H2O	N2O	NH3	O3	SO2	NO2
Benzene	4.605503	0.005244	0.381283	-0.18403	0.228199	-0.00127	-0.01177	-0.15869	2.851475	-0.47747	0.0088
CH4	-0.00023	5.059205	0.000265	-0.00528	-0.93713	4.27308	3.706554	-0.0043	-7.47E-05	-0.61649	0.764108
CO2	0.575985	0.044047	3.557787	-0.89717	-0.46921	-0.09388	0.06099	1.317211	0.15795	-1.40068	-0.64139
F12	-0.03602	-0.4132	-1.94532	3.750212	-0.04478	-1.00813	-0.46851	1.301645	-0.0071	0.770576	-1.14425
F114	0.822751	-1.40773	0.320234	-0.31927	4.225587	-0.75816	-1.0849	-0.21543	1.685449	1.19626	1.078435
H2O	-0.02101	4.084221	-0.01131	-0.13509	-0.31626	9.828254	4.691056	-0.07424	0.004298	0.030634	0.2209
N2O	0.000149	3.745976	0.000459	0.000207	-0.47218	4.937586	4.857501	-0.0564	0.000302	-0.02032	0.945458
NH3	-0.13954	-0.06865	0.455681	1.929612	-0.6289	-0.26042	-0.09207	9.181502	-1.18378	-0.57819	-1.05735
O3	3.237334	-0.00831	0.50113	-0.48662	0.806284	-0.02597	-0.01786	-0.21108	3.443482	-0.89613	-0.00054
SO2	-0.04006	-1.65637	0.027122	0.241203	1.968923	-1.4417	-1.70067	-1.22598	0.001221	3.214478	-0.02642
NO2	-0.00873	1.607151	-0.30641	-1.77754	0.460347	0.862788	1.572681	-1.04842	0.099872	-0.51736	3.944278

A graphic visualization of this matrix is given in Figure 9.

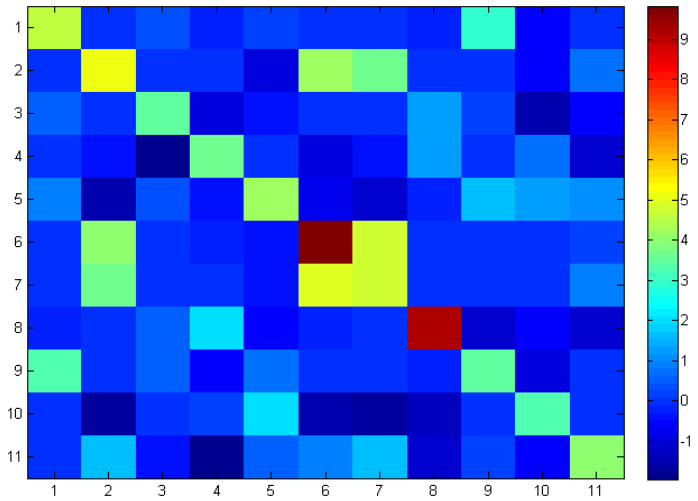

Figure 9. Graphic visualization of Table 1

We note two facts concerning this matrix:

1. There is no single number which appears appropriate towards setting a threshold. For example, the shift score NH_3 gets on a pixel containing itself is a factor of 3

higher than other gases. NH_3 has evidently a unique signature which will be hard to imitate.

2. For a pixel with O_3, Benzene gets a score of 3.2 while O_3 itself gets only slightly higher, i.e. 3.4. Apparently, one gas can be confused with another if they are similar enough.

We suggest the following: for the gases tested here, we should always give the highest shift score to a pixel which looks like itself; to check if a gas is there we will compare the score it got to the score it gets for a pixel which looks like itself. The graphic interpretation for this is that the highest score in any column is the diagonal; we will compare our result to the value obtained on the diagonal.

In addition, when checking for the presence of gasses, the highest score received is almost always by the actual gas which is present. (Any deviation from this is due to the preprocessing we do of the gas pixel (see N_2O/H_2O); this subject is under investigation). Although H_2O may get a very high score for itself compared to the score CO_2 got for itself, it won't get a higher score on a pixel which looks like CO_2 than the gas CO_2 itself got. The graphic interpretation for this is that the highest score in any row is the diagonal.

Thus, for our PLT measurement in our shift algorithm, we will compare the shift score which we get to the shift score that the gas would get for a pixel which looks like itself.

To fix the problem of gases resembling one another we propose the following: for any two gases in the fit after the initial basic result (including the first Shift algorithm), we will check the above table to see if they could have been confused one for the other (that gas A gets a high shift score for a pixel which looks like gas B). If they could, then unless the gasses got extremely high shift scores (in which case we will be forced to say both gases are present) we will choose the one which got a higher shift score (compared to itself).

The algorithm:

0. Run the initial step-wise algorithm and determine which gases are possibly present in the pixel.

1. Run the Shift algorithm and create shift results for all gases found.

2. For each gas found for every pixel, check the shift result; if it is not 30% of the shift result that the gas would get on a pixel which looks like itself (the diagonal in the above table), remove the gas from our fit.

3. For every pair of gases found, check the above table to see if these are a problematic pair. If gas A fitted on a pixel which looks like gas B gets a shift result of at least 30% compared to B fitted on B AND vice versa then:

3.a. If both shift scores for the gases were at least 60% of the score the gas got for itself, then keep both gases in the fit.

3.b. Otherwise, remove the gas whose ratio: (shift score gas obtained on pixel)/(shift score gas gets for itself) is lower.

4. If only gas A gets high results for B but not the other way around, then the fact that we found both points strongly to the fact that it was only gas A. And so, unless B got a score of 60% compared to itself, remove gas B out of the fit.

5. FINAL RESULTS:

After implementing the above algorithm on both data sets we received for the TELOP cube the results shown in Fig. 10, and the results for the DIRSIG cube in Figure 11.

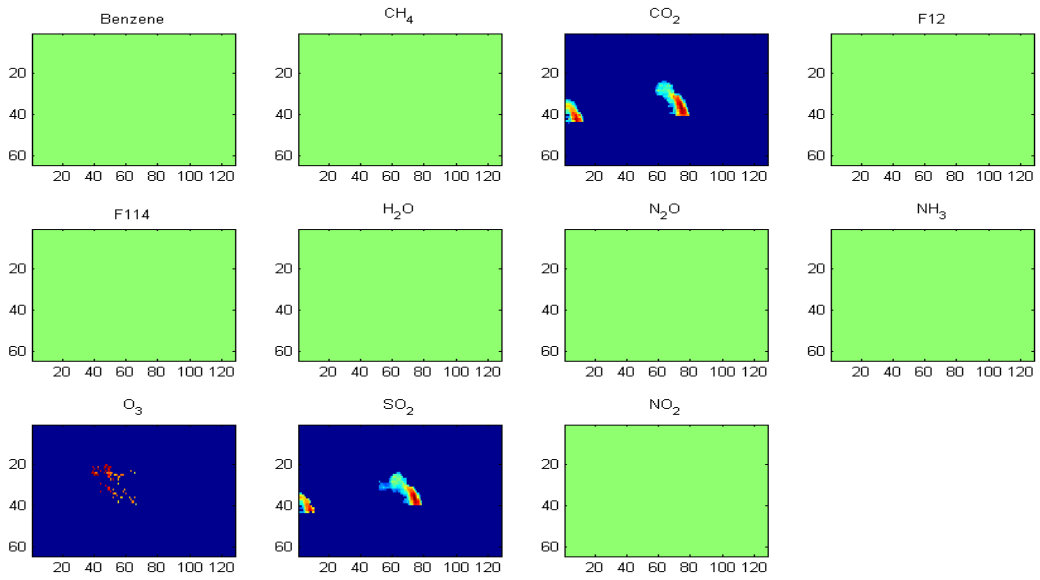

Figure 10. Final results for TELOP cube after gas elimination process

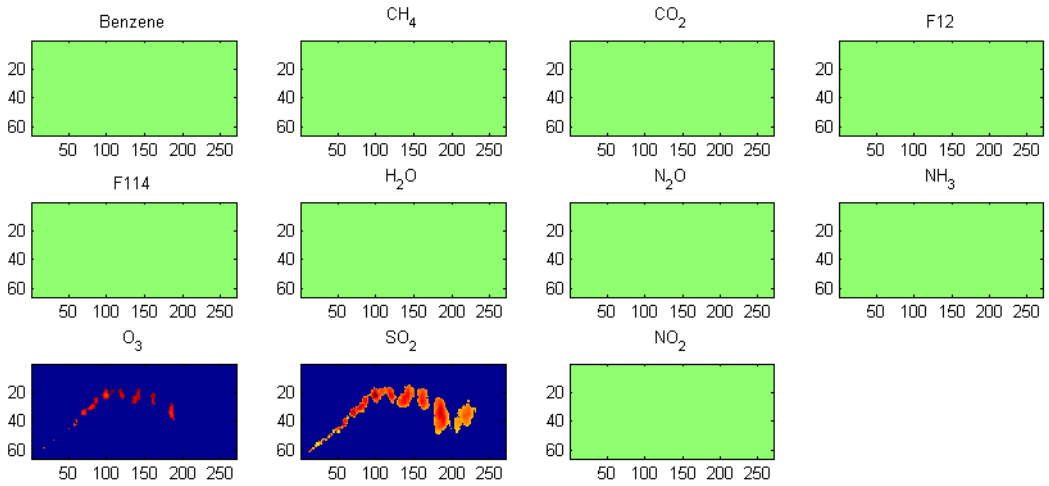

Figure 11. Final results for DIRSIG

6. CONCLUSIONS:

An extension of our algorithm for the stepwise detection of gases is considered. In particular, we tackle the problem of gases which resemble other gases, i.e., often when gases a and b are detected in a gas cloud, only a is present, while b simply looks like a. In our new algorithm, a prior analysis shows which gases can be confused with each other; thresholds are set to avoid multiple gas identifications of a single gas.

Obviously, the establishment of accurate thresholds needs testing on multiple datasets. Future work will be dedicated to expanding on additional experimental results.

REFERENCES

[1] Pogorzala, D. R., Messinger, D. W., Salvaggio, C., and Schott, J. R., "Gas plume species identification by regression analyses," Proc. SPIE 5425, 583-591 (2004).

[2] Klil-Horesh, O., "Separating concentration and temperature dependencies in gas plume absorption coefficients," M.Sc. thesis, Ben-Gurion U., Dept. of Electro-optics (2010).

[3] Feinmesser, Y. and Rotman, S. R., "Iterative approach for gas detection and identification," Proc. IEEE 26th Convention of Electrical and Electronics Engineers in Israel, 73-76 (2010).

ACKNOWLEDGEMENTS

We thank Mr. Lior Sagiv for assistance in the taking of the original image with the TELOPS camera and Mr. Yoav Feinmesser with help in the development of the original shift algorithm in the stepwise regression technique. This work was supported by an EOARD grant, funded by the U.S. Air Force.